Biological Investigation of a Water-Soluble Isoginkgetin-Phosphate Analogue, Targeting the Spliceosome with In Vivo Antitumor Activity

Boris Letribot, Megane Nascimento, Giulia Cerrato, Romain Darrigrand, Valerie Salgues, Dolor Renko, Alain Pruvost, Mouad Alami, Samir Messaoudi, Sebastien Apcher

Biological Investigation of a Water-Soluble Isoginkgetin-Phosphate Analogue, Targeting the Spliceosome with in Vivo Antitumor Activity

Boris Letribot,[a] Megane Nascimento,[b] Giulia Cerrato[c], Romain Darrigrand,[b] Valerie Salgues[b], Dolor Renko,[a] Alain Pruvost[d], Mouad Alami [a] Samir Messaoudi [a,]* and *Sebastien Apcher[b,*]*

Affiliations:

[a.] Université Paris-Saclay, CNRS, BioCIS, 92290, Châtenay-Malabry, France

[b.] Université Paris-Saclay, Institut Gustave Roussy, Inserm, Immunologie des tumeurs et Immunothérapie, 94805, Villejuif, France.

[C.] Université Paris-Saclay, Institut Gustave Roussy, Metabolomics and Cell Biology Platforms, , 94805, Villejuif, France.

[d.] Université Paris-Saclay, CEA, INRAE, Département Médicaments et Technologies pour La Santé, SPI, 91191, Gif-sur-Yvette, France

ABSTRACT

The first total synthesis of the natural product isoginkgetin as well as four water-soluble isoginkgetin-phosphate analogues are reported herein. Moreover, the full study of the **IP2** phosphate analogue with respect of pharmacological properties (metabolic and plasmatic stabilities, pharmacokinetic, off-target, etc.) as well as *in vitro* and *in vivo* biological activities are disclosed herein.

INTRODUCTION

Recent advances in oncology are related to the advent of immunotherapy, one of the most promising lines of research targeting the immune system. The increased understanding of the complex interactions regulating the immune system has contributed to the pharmacological activation of antitumor immunity. Approved T cell checkpoint inhibitory antibodies[1] such as ipilimumab (anti-CTLA4), atezolizumab (anti-PDL1), pembrolizumab, and nivolumab (anti-PD1) are currently part of approved therapeutic interventions for treating patients with various malignancies. The success of these biologics in the clinic is now inspiring the discovery and development of small molecule drugs (SMDs), either chemically synthesized or isolated from natural sources able to act on intracellular targets affecting immunomodulatory pathways in cancer. Modulation of the immune system with SMDs might offer the following advantages: (*i*) possible complementarity and synergism to biologics; (*ii*) easier production compared with immunotherapeutic biologics; (*iii*) cost-cutting; (*iv*) straightforward patient

access than biological immunotherapies; (*v*) potential oral bioavailability; (*vi*) greater exposure levels inside the tumor microenvironment; (*vii*) better opportunities to tackle intracellular targets not accessible to biologic agents.

Thalidomide (Figure 1A), a glutamic acid derivative, and its analogues (*e.g.*, lenalidomide and pomalidomide, Figure 1A) have gained attention thanks to the discovery of their immunomodulatory properties. Although the exact mechanism of action remains unclear, it has been shown that thalidomide exhibits a wide range of cellular actions including a strong inhibition of TNF-α factor[2], stimulation of T- and natural killer cells,[3] and decrease in plasma cell adhesion to stroma, reducing cytokine production and promoting apoptosis.[4] However, due to several adverse effects, mainly a teratogenic effect, the clinical use of thalidomide was limited. In recent years, there is an increased interest in the discovery of SMDs targeting the same pathways of immune checkpoint inhibitors monoclonal antibodies (CTLA4, PD-1, PD-L1)[5], as well as less validated targets, by exploring novel approaches (modulation of the immune response, trafficking to the tumor microenvironment, cellular infiltration, tumor cell-based vaccines, etc.). A remarkable example of such approaches is the identification of SMDs targeting tumor antigens in order to enhance the immune response against cancer cells.
Antigen presentation, mediated by major histocompatibility complex (MHC) class I molecules, is a fundamental process for the specific immune responses. While the molecular mechanisms of antigen presentation pathways have been studied extensively, knowledge about the origin of antigenic peptides has continued to evolve. Some years ago, it has been suggested that a major source of peptides presented by the MHC class I pathway was derived from the degradation of so-called Defective Ribosomal Products (DRiPs).[6] Our major contribution on this pathway was made in 2011 and 2013, when we demonstrated that antigen presentation is equivalent whether the precursor peptide is expressed from an intron or an exon, and could be supported by the so-called Pioneer Translation Products (PTPs).[7] Overall, we have demonstrated that PTPs, being the major source of antigenic peptides for the MHC class I pathway derived, to a larger extent, from non-canonical translation events that take place during the early scanning of newly synthesized mRNAs.

Polyphenolic biflavonoids are gaining increasing recognition as modulators of physiological and pathological responses. Among them, the natural product isoginkgetin isolated from the leaves of the *Ginkgo biloba* tree (Figure 1B) has been associated with a variety of biological activities, including antitumor and anti-inflammatory effects.[8] Isoginkgetin also exhibited antineoplastic properties by impairing the production of matrix metalloproteinase-9 *via* inhibition of the NF-κB pathway.[9] Recent studies reported that isoginkgetin inhibits the chymotrypsin-like, trypsin-like, and caspase-like activities of the 20S proteasome and impairs NF-κB signaling, suggesting that isoginkgetin may display its biological activity in part through proteasome inhibition.[8a] Another key biological activity associated with isoginkgetin is the inhibition of mRNA splicing.[10] Indeed, isoginkgetin is a well-known spliceosome inhibitor, which prevents the recruitment of U4/U5/U6 ribonucleoprotein (snRNP), and thus blocks the transition from complex A to a stable complex B[10, 11]. O'Brien *et al.* also showed that isoginkgetin induces the accumulation in the nucleus of pre-mRNAs from different endogenous transcripts encoding (*e.g*., actin or β-tubulin) and report that splicing inhibition is the mechanistic basis of the anti-tumor activity of this molecule.[10] Finally, in an attempt to

support and define more accurately the PTPs pathway, we have shown that isoginkgetin positively modulates the surface presentation of a PTP-derived model antigen in healthy cells treated with this compound. In line with this finding, we recently reported for the first time, that isoginkgetin and its phosphate analogue **IP2** (Figure 1B) act at the production stage of the PTPs, which are polypeptides synthesized from unspliced mRNA[12]. In addition, we showed that **IP2** acts as an immunomodulatory agent that increases PTP-derived antigen presentation in cancer cells *in vitro* and impairs tumor growth *in vivo* much more efficiently than isoginkgetin. These results clearly suggest that the spliceosome is a druggable target, capable of rendering tumor cells more visible to tumor-infiltrating T lymphocytes (TILs). Herein, we report for the first time the total synthesis pipeline of isoginkgetin as well as the synthesis of a water-soluble phosphate analogues, the full study of the phosphate **IP2**, optimization, characterization, stability, and additional *in vitro* and *in vivo* biological activity.

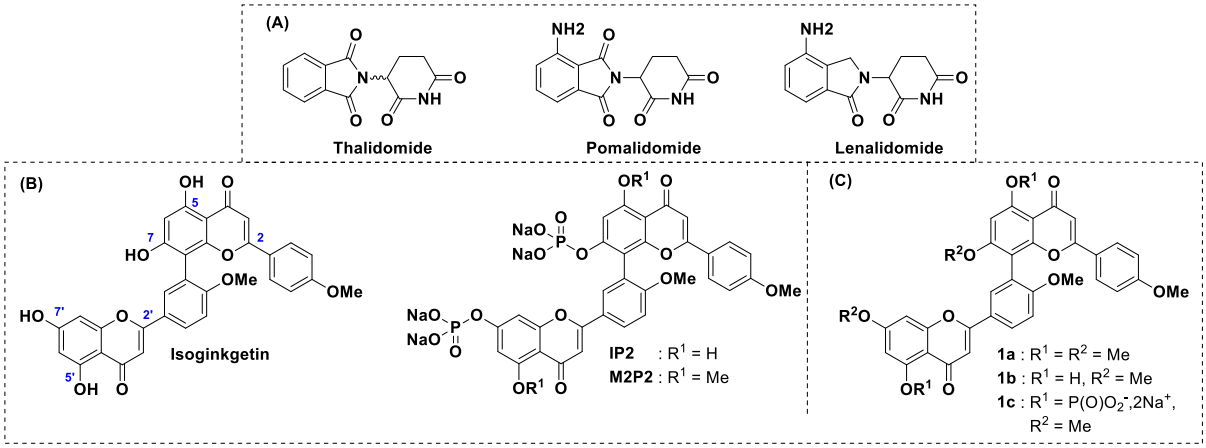

Figure 1: (**A**) Structure of thalidomide and its analogues, (**B**) isoginkgetin, phosphates **IP2** and **M2P2**, (**C**) structure of the designed analogues **1a-c**.

RESULTS AND DISCUSSION

Chemistry. Due to the limited natural abundance of isoginkgetin and considering its exorbitant cost (1 g/4 000 €), the total synthesis of the molecule would be of great interest. Moreover, from a synthetic point of view, this is a highly challenging task since no total synthesis has been described in the literature so far. Thus, we report our success in developing the first synthetic approach toward isoginkgetin as well as the preparation of synthetic analogues **1a-c** (Figure 1).

As outlined in Scheme 1, the key step toward isoginkgetin synthesis involves the assembly of the electrophilic partner iodoflavone **6** and the nucleophilic partner flavonyl boronic ester **14** under palladium catalysis (Scheme 1). On one hand, the preparation of the first key intermediate iodoflavone **6** was accomplished in a three-step sequence starting from commercially available phlorogucinol. Briefly, acacetin **4** which was prepared under reported conditions[13] was transformed in its benzyl-protected analogue **5** followed by a selective iodination in the presence AgOTf/I_2 at 0°C[14] leading to the desired iodoflavone **6** in 62% yield (Scheme 1).

On the other hand, the second key intermediate **14** was prepared through a multi-step sequence starting from two simple building blocks THAP and 4-methoxybenzaldehyde (Scheme 1). The compound **10** was prepared as previously reported[15] by using a

protection/deprotection sequences starting from a (*i*) selective MOM-protection of the non-chelated phenolic hydroxyl groups of phloroacetophenone (THAP) to provide **7**, (*ii*) Benzyl-protection of the remained -OH group to furnish **8**, (*iii*) removal of the two MOM-groups with hydrochloric acid, and then (*iv*) regioselective benzylation under classical conditions. Accordingly, this four-step sequence leads to compound **10** in an overall yield of 34% (4 steps). The second building block; the iodinated intermediate **11** was readily obtained inn 79% from 4-methoxybenzaldehyde using ICl in AcOH at 60 °C. The assembly of compounds **10** and **11** was achieved *via* a Claisen-Schmidt reaction to produce the chalcone **12**, which was cyclized in the presence of catalytic iodine (as the oxidant) in DMSO at 110 °C into the benzyl-protected flavone **13** in an excellent yield of 93% (Scheme 1). Borylation of this later under classical Miyaura borylation reaction yielded the nucleophilic partner flavonyl boronic ester **14** in a moderate 47% yield (Scheme 1).

As the last step, a Pd-catalyzed Suzuki-Miyaura cross-coupling of iodinated compound **6** with borylated derivative **14** was conducted in the presence of NaOH as the base in DMF/H_2O. Accordingly, the expected benzylated-isoginkgetin **15** was isolated after column chromatography purification in 40% yield. Finally, removal of Benzyl groups through a hydrogenation step furnished isoginkgetin in 75 % yield (30 % yield over two steps). The exact structure of the synthesized isoginkgetin was confirmed unambiguously by the comparison of NMR data with the commercial (natural) compound.

Scheme 1: Synthetic Pathway for Isoginkgetin.

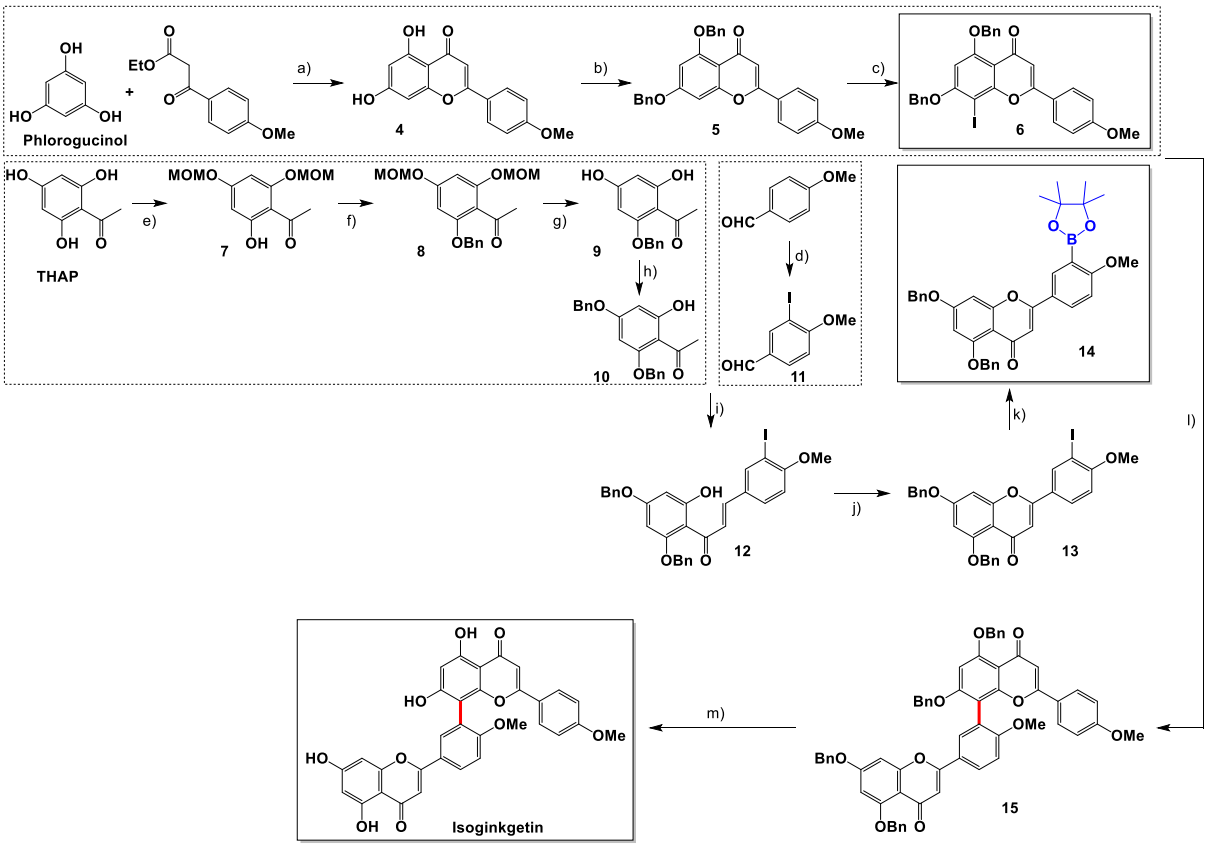

a) Ethyl 4-methoxybenzoyl acetate (1.6 eq.), DMAP (0.08 eq.), 200°C, 3h; b) BnBr (2.7 eq.), K_2CO_3 (2.7 eq.), DMF, 16h, t.a. ; c) I_2 (1.05 eq.), AgOTf (1.2 eq.), DCM, 0°C, 1.5 h; d) ICl (2 eq.), AcOH, 80 °C, 24 h ; e) MOMCl (2.1 eq.), DIPEA (2.1 eq.), DCM, 0°C->t.a., 4 h; f) BnCl (1.2 eq.), K_2CO_3 (1.5 eq.), DMF, 80°C, 5 h; g) HCl(aq.) (2N)/MeOH, 100 °C, 1 h; h) BnCl (1.05 eq.), K_2CO_3 (1.05 eq.), DMF, t.a., 16h; i) NaH (1.2 eq.), DMF, 0°C->t.a., 16h; j) I_2 (0.05 equiv.),

DMSO, 100 °C, 16h; k) Bis(pinacolato)diboron, $PdCl_2$(dppf), KOAc, DMF, 80 °C; l) $Pd(PPh_3)_4$, NaOH, DMF: H_2O (9:1), 80°C, 4 h; m) Pd/C, $Pd(OH)_2$/C, H_2, MeOH/DCM.

In order to examine the importance of the phenolic functions at C5/C5' and C7/C7' positions of isoginkgetin on the biological activity, the synthesis of a series of analogues starting from isoginkgetin was envisioned (Scheme 2). The first modification which was achieved concern the partial or total methylation of the natural product by using methyl iodide as the methylating agent in the presence of K_2CO_3. Thus, running the reaction of isoginkgetin with an excess of methyl iodide provided **1a** in 94% yield, however the use of 2 equiv. of methyl iodide led to the tetra-*O*-methylated isoginkgetin **1b** in 88% yield and excellent selectivity. This regioselectivity may be explained by the different reactivities between the phenols at C5/C5' *versus* C7/C7'. In a similar way, selective phosphorylation employing diethylchlorophosphate provided selectively the diphosphate analogue **2** which was finally *O*-methylated under classical conditions to furnish the orthogonally protected compound **3** in good yield.

Scheme 2: Synthetic Scheme for Biflavonoids **6a-c** and Isoginkgetin Phosphate Analogue **IP2**.

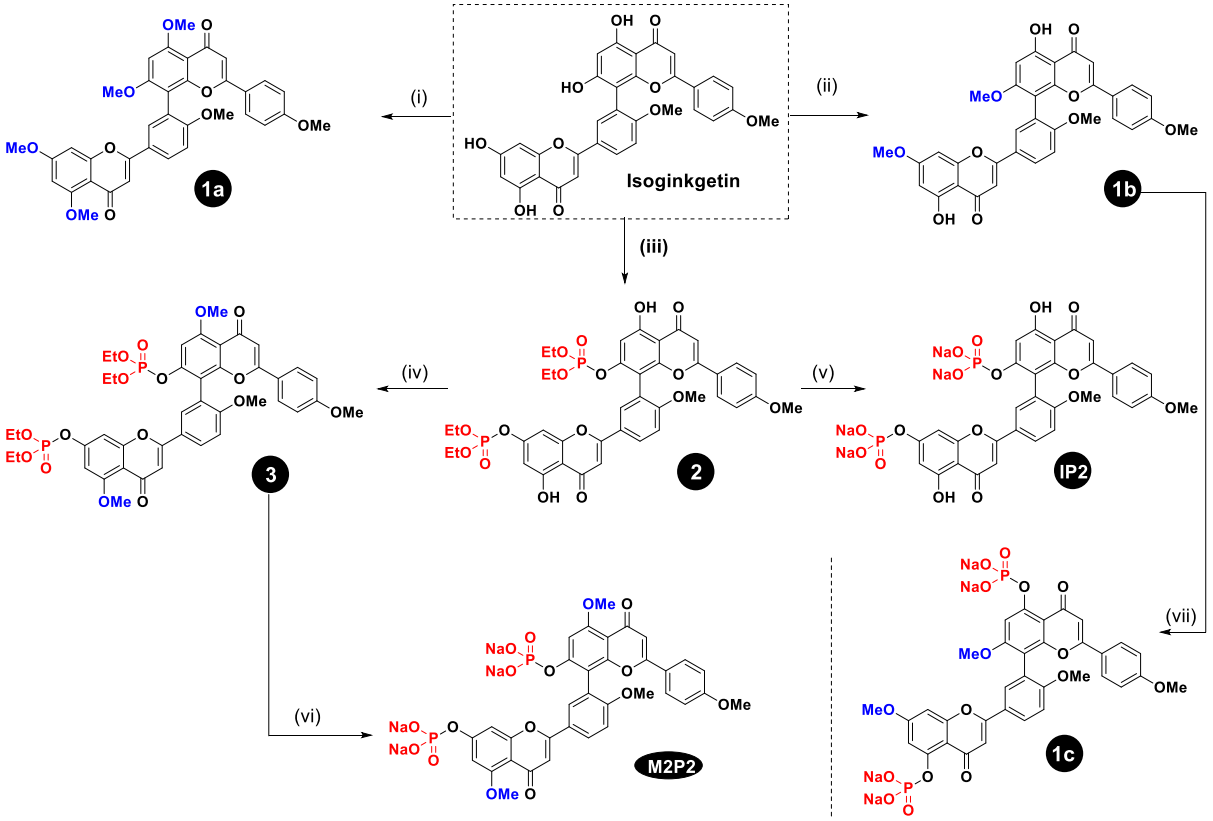

Reagents and conditions: (i) MeI (7 equiv), K_2CO_3 (5 equiv), DMF, 20 °C, 20 h, 94%. (ii) MeI (2 equiv), K_2CO_3 (2.5 equiv), DMF, 20 °C, 20 h, 88%. (iii) KOH (8 equiv), H_2O, $(EtO)_2POCl$ (2.2 equiv), TBAB (2 equiv), CH_2Cl_2, 20 °C, 2 h, 77%. (iv) MeI (3 equiv), K_2CO_3 (5 equiv), DMF, 20 °C, 20 h, 97%. (v) TMSBr (40 equiv), CH_2Cl_2, 20 °C, 30 min, then NaOH (4 equiv), H_2O, 20 °C, 20 h, 96%. (vi) TMSBr (40 equiv), CH_2Cl_2, 20 °C, 16 h, then NaOH (4 equiv), H_2O, 95%. (vii) (a) NaH (5 equiv.), $(EtO)_2POCl$ (4 equiv), THF, 20 °C, 30 min; (b) TMSI (8 equiv), CH_2Cl_2, 20 °C, 30 min, then NaOH (4 equiv), H_2O, 77%.

One of the main limitations of this series of analogues for further *in vivo* studies is their poor water solubility. In order to increase their solubility and avoid the use of toxic carriers or co-solvents (*e.g.*, DMSO), we proposed to prepare the phosphate salts starting from the previously synthesized isoginkgetin and intermediate **1b** bearing free phenol groups. Thus,

starting from compound **2**, deprotection of the ethyl ester groups with TMSBr furnished the phosphoric acid intermediate, which was immediately transformed to the disodium phosphate analogue **IP2** in the presence of sodium hydroxide. The use of TMSBr instead of TMSI has several desirable features, such as high yield, a clean and reproducible protocol, short reaction time, and easy purification of **IP2**. As expected, the **IP2** analogue showed higher water solubility (≥ 27 mg/mL) than the parent compound isoginkgetin (< 0.5 mg/mL). By the same strategy, the sodium phosphate salts **M2P2** and **1c** were readily prepared in good yields from their intermediates **3** and **1b**, respectively.

Biological Results.

Immunomodulatory activity. Synthetic analogues **1a, 1b** and **1c** (Figure 1), prepared from isoginkgetin, have been tested *in vitro* for their ability to increase the MHC-I presentation of PTP-derived antigens *in vitro* and compared to **IP2**. For that purpose, murine MCA205 fibrosarcoma cells transiently expressing the intron-derived SL8 epitope within the β-Globin gene construct (globin-SL8-intron) were treated with increasing doses of compounds **1a, 1b and 1c**. As depicted in Figure 2, none of the biflavonoids did cause an increase in antigen presentation whereas **IP2** elicited an increase in the intron-derived SL8 antigen presentation, as already shown in a previous study.[12] These results highlight the importance of the phenolic functions in C5/C5' and C7/C7' positions for the immunomodulatory properties of the molecule.

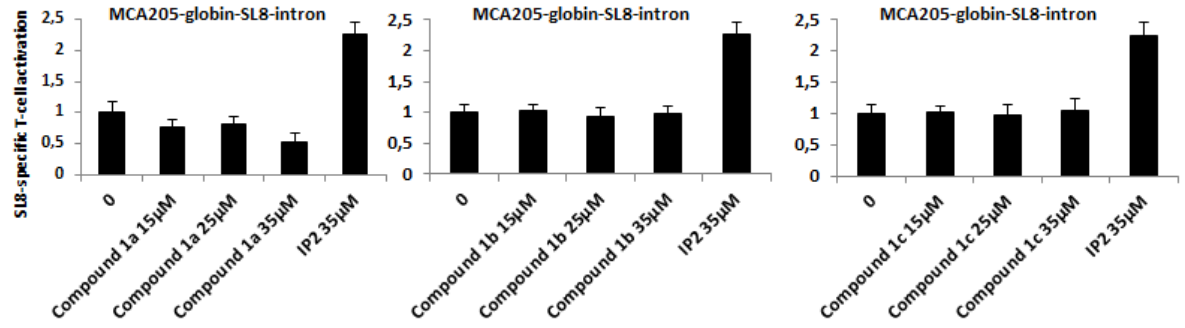

Figure 2: *In vitro* effect of splicing inhibition on PTP-antigen presentation. Activation of B3Z cells after recognition of the SL8 peptide on the surface of MCA205 fibrosarcoma cells upon treatment with biflavonoids **1a, 1b and 1c** at 15, 25 and 35 µM and IP2 at 35 µM. This result is representative of at least 3 independent experiments.

In Vitro Antiproliferative Activity. The antiproliferative activity of IP2 was assessed in a MTT(dimethylthiazol-diphenyltetrazolium bromide)- based colorimetric assay. Results depicted in Figure 3 demonstrate that **IP2** did not show any growth inhibition at 10 µM on a series of human cancer cell lines (MCF-7, A549, HCT116, K562, K562R). However, the MCA205 mice fibrosarcoma and the HUVEC cell lines demonstrated a decrease in cell viability following exposure for 72 h, of 20% and 25% respectively. Spliceosome inhibitors have only been exploited so far for their cytotoxic activity directed toward tumor cells bearing alteration of their splicing machinery. We demonstrate here that by modifying the Isoginkgetin molecule, we have succeeded in making the IP2 derivative non-cytotoxic for cancer cells while keeping its spliceosome inhibitory activity and its immunomodulatory activity intacts.

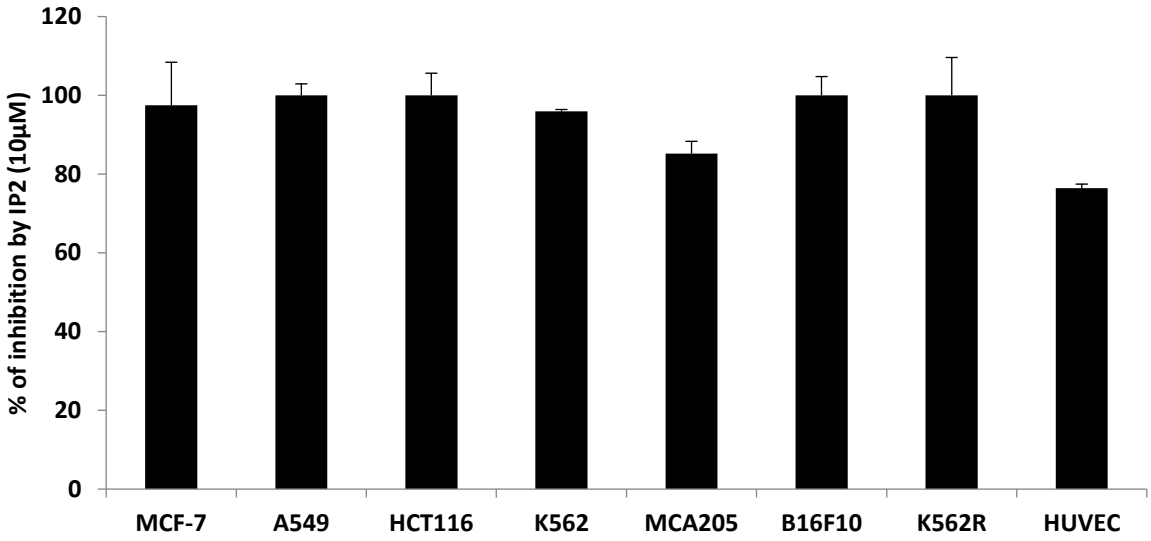

Figure 3. Effects of **IP2** on viability at a concentration of 10 µM on a panel of cancer cell lines using a MTT assay.

*Druglike Profile of **IP2***. Human and mice liver microsomes are extensively used in the pharmaceutical industry in *in vitro* drug metabolism assays to evaluate the ADME properties of drugs in development. Since phosphate analogue **IP2** exhibited *in vitro* immunomodulatory properties, increasing PTP-derived antigen presentation in fibrosarcoma and melanoma cancer cell lines, its druglike profile was evaluated. Metabolic stability of **IP2** was expressed as the percentage (%) of the remaining parent-compound concentration over time, as well as kinetic monitoring was performed by HPLC-MS/MS after incubation (45 min) with mice liver microsomes (MLM) and human liver microsomes (HLM). We demonstrate that **IP2** is poorly metabolized by MLM (17.7%), whereas its incubation with HLM induced a weak metabolization of 39.2% (Table 1). The percentage of metabolic stability at 45 min is very close with or without NADPH, clearly suggesting that the weak metabolization of **IP2** is not due to CYP450s but probably to other enzymes. Other druglike profile evaluations revealed that in addition to its low intrinsic clearance, **IP2** was stable in the plasma of mice and humans after an incubation time of 2 h (> 96%), and was extensively (> 98%) bound to plasma protein (Table 1).

Table 1. *in vitro* liver microsomes stability assay, plasma stability assay, and plasma protein binding assay of **IP2**

	Metabolic stability			Plasma stability up two hours	Plasma protein binding[a]	
	(%)	non-NADPH dependent (%)	Cl_{int} µL/min/mg protein	(%)	f_u index	protein binding (%)
Mice	82.3	72.4	8.0	98.1	0.02	98.1
Human	60.8	64.7	11.0	94.1	0.02	98.3

[a]*For the method used to determine the plasma protein binding, see the experimental section*

*Selectivity of **IP2** against Other Receptors and Enzymes.* *In vitro* pharmacological profiling is extensively used in the drug discovery process to identify undesirable off-target activity profiles that could hinder or halt the development of a candidate drug. In this context, the evaluation of **IP2** specificity using highly relevant and predictive functional tests would provide more informed data on its safety. Ligand profiling was performed to screen the binding affinities of **IP2** against a broad range of targets (DiscoverX, Safety47^{TM} panel) including nuclear hormone receptors, ion channels, transporters, kinome scan binding, GPCR cAMP modulation, calcium mobilization, and other enzymes, which would be beneficial to rule out other non-target activities. Among 47 targets examined with **IP2** at 10 µM concentration, we set a threshold of 25% for inhibition of activity on all tested targets as summarized in Table 2. Preclinical safety screens indicated that **IP2** was interacting with three G-protein coupled receptor ADRB1 (35%), HRH2 (40%) and OPRD1 (53%). Moreover, **IP2** inhibited the following three enzymes: COX1 (52.8%), PDE3A (84.8%) and PDE4D2 (87.2%) but did not reveal any inhibition activity of ion channels including, hERG potassium channel found in the heart using an automated patch clamp electrophysiology measurement in CHO-hERG cells. The absence of hERG ion channel currents inhibition by **IP2** was confirmed using a manual patch clamp electrophysiology assay on HEK293 cells. Indeed, **IP2** did not inhibit hERG ion channel currents at all concentrations tested (from 0.01 up to 50 µM), suggesting that **IP2** could be used as a promising candidate for further development.

Since the exact mechanism of **IP2** by which it enhances the adaptative immune response against tumor antigens is unknown, and due to the observed level of inhibition of the two phosphodiesterases isoforms PDE3A and PDE4D2, we questioned whether PDEs could represent potential molecular targets of **IP2**. Consequently, Zardaverine, a well-known dual-selective PDE3/4 phosphodiesterase inhibitor[16] was tested for its ability to increase the MHC-I presentation of PTP-derived antigens *in vitro* in comparison with **IP2**. For that purpose, the murine MCA205 sarcoma transiently expressing the intron-derived SL8 epitope within the β-Globin gene construct (globin-SL8-intron) were treated with increasing doses of zardaverine for 18h. While treatment with **IP2** (15 µM) increased the intron-derived SL8 presentation in MCA205 as expected, Zardaverine had no effect on antigen presentation in this cell line (Figure 4)

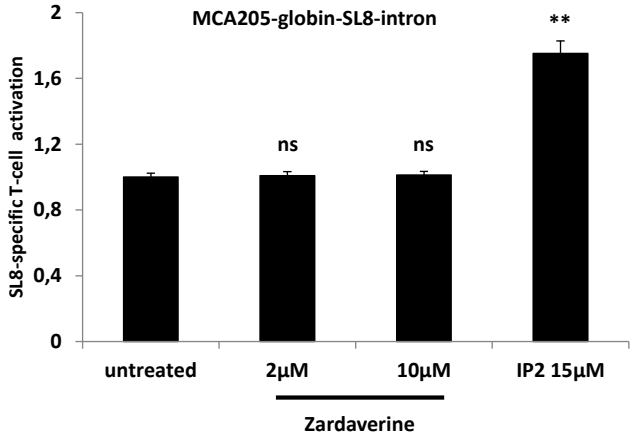

Figure 4: Zardaverine, a specific PDE inhibitor, has no effect on antigen presentation. SL8-specific B3Z T cell activation after co-culture with MCA205 fibrosarcoma transiently expressing the intron-derived SL8 epitope and treated for 18h with Zardaverine or IP2 at indicated doses. Unspecific B3Z T-cell

activation was considered to normalize the results. Data are means ± SEM of relative B3Z T-cell activation for at least three biological replicates. Each value was compared to the control, and the *P*-value was calculated with Student's *t*-test: **p<0.01.

Table 2. Eurofins Safety screening Selected Results of **IP2** (10 µM) against Various Targets

Target Type	Target Name	Assay Mode	% Inhibition
GPCR	ADRB1	antagonist	35.0
GPCR	HRH2	antagonist	40.0
GPCR	OPRD1	antagonist	53.0
enzyme	COX1	inhibitor	52.8
enzyme	PDE3A	inhibitor	84.8
enzyme	PDE4D2	inhibitor	87.2

*Pharmacokinetic Profile of **IP2.*** Next, biflavonoïd **IP2** was profiled in two species, mice and dogs for PK parameters. As illustrated in Table 3, **IP2** exhibited a modest pharmacokinetic profile in mice, with a low clearance and half-life but displayed a high bioavailability. IP2 presented a very low clearance in dogs and a moderate half-life of elimination.

Table 3. Pharmacokinetic Profile of **IP2**.[a]

	Dose (mg/kg)	C_{max} ng/mL	T_{max} (h)	$T_{1/2}$ (h)	CL (ml/min/Kg)	*F* (%)	$MRT_{(0\text{-}t)}$ (h)	AUC_{tot} ng/mL*h	AUC_{extra} (%)
ip mice	9.103	2078	0.0833	0.8	154	86	0.7	982.3	1.3
iv mice	0.711	322.7	0.0833	1.1	133	-	0.9	88.8	15.2
iv dog	26.76	272(µg/mL)	0.0833	3.8	0.69	-	3.8	654.7 (µg/mL*h)	0.9

[a] IP2 was administrated intravenously (*iv*) or intraperitoneally (*ip*). For mice: *Single administration by IV and IP routes in male C57BL/6J mice. Blood samples were taken from the tail vein under sodium heparin for plasma preparation. Blood sampling (12 mice/administration route): 3 same mice at 0.083 h and 2 h, 3 others at 0.25 h and 4 h, 3 others at 0.5 h and 8 h and 3 mice at 1 h and 24 h. For dogs: Single administration by IV route in male beagle dog. Blood samples were taken from the jugular vein under K2 EDTA for plasma preparation. Blood sampling (3 dogs): Predose, 0.083 h, 0.25 h, 0.5 h, 1 h, 2 h, 4 h, 6 h, 8 h and 24 h.* [b] $T_{1/2}$, half-life of elimination. [c] C_{max}, maximum plasma concentration achieved. [d] $AUC_{(0\text{-}t)}$, total exposure following single dose. [e] CL, total clearance. [f] *F*, bioavailability, MRT, mean residence time, AUC_{extra}, percentage of exposure extrapolated between t (last observed concentration) and ∞.

Isoginkgetin and IP2 do not induce immunogenic cell death hallmarks in human cancer cells in vitro. Depending on its ability to activate an adaptive immune response, regulated cell death can be classified into two categories: immunogenic cell death (ICD) and non-immunogenic cell death.[17] As a host defense approach, cells infected with viruses or intracellular bacteria undergo ICD-mediated release of antigens, which stimulates immune response to eliminate pathogens. The innate and adaptive immune response can only be effective if tumor cell death is immunogenic via the secretion or exposure of damage-associated molecular patterns (DAMPs) and the production of type I IFNs. Altogether these will participate in the recruitment and maturation of DCs which will then be able to pick up antigens from the extracellular environment and load them onto MHC class I and II. The major effect of ICD involves the

release, secretion, or exposure of multiple DAMPs including calreticulin (CALR), adenosine triphosphate (ATP), high mobility group box 1 (HMGB1), type I interferon (IFN) and annexin A1 (ANXA1).[18] Multiple approaches have been shown to elicit ICD, including physical interventions such as radiotherapy or high hydrostatic pressure, and also chemotherapy. Indeed, the very first drug demonstrated to trigger ICD was the anthracycline doxorubicin and since, different chemotherapeutic agents followed, including, but not limited to, oxaliplatin, cyclophosphamide and mitoxantrone.[17] In our context, since IP2 is able to induce a specific immune response *in vivo* by inhibiting the spliceosome, we wonder whether this specific anti-cancer immune response could also be, in part, due to the ability of IP2 to induce ICD. To evaluate the ICD activity of the splicing inhibitors Isoginkgetin and **IP2**, different parameters of ICD hallmarks were measured by robotized epifluorescence microscopy followed by automated image analysis. For that purpose, Isoginkgetin and **IP2** were compared to different confirmed ICD inducers such as mitoxantrone (MTX), oxaliplatin (OXA) and dactinomycin (DACT). Given that most ICD inducers were recently shown to inhibit DNA-to-RNA transcription[19, 20], we firstly assessed the inhibition of RNA synthesis in human osteosarcoma U2OS cells by means of multiple techniques. Unlike DACT, a well-known inhibitor of transcription, and the two common ICD-stimulatory chemotherapeutics MTX and OXA, isoginkgetin and **IP2** were not endowed with the ability to inhibit transcription. Indeed, when cells were cultured in the presence of the alkyne-modified nucleoside, 5-ethynyl uridine (EU), isoginkgetin and **IP2** failed to reduce its incorporation into treated cells as revealed by click chemistry (Figure 5A and suppl. Figure S1). Furthermore, isoginkgetin and **IP2**-treated cells were not classified as bearing a transcription inhibition phenotype, neither when a deep-learning algorithm was applied on cells imaged in transmitted light (Figures 5A and B),[21] nor on fluorescent RNA-stained cells (Figures 5C and D). We next investigated whether Isoginkgetin and **IP2** have the capacity to stimulate the release of ATP from U2OS-treated cells by measuring the decrease in the cytoplasmic fluorescence of ATP-containing vesicles stained with the fluorescent probe quinacrine. As shown in Figures 5E and F, while both classical ICD inducers MTX and OXA caused the reduction of quinacrine fluorescence staining of U2OS-treated cells, isoginkgetin and IP2 did not show any decrease in ATP signal. Moreover, U2OS cells engineered to express a CALR-green fluorescent protein (GFP) fusion protein or an HMGB1-GFP fusion protein, were treated with the different ICD inducers, and with isoginkgetin and **IP2**. While MTX and OXA caused an accumulation of CALR-GFP fusion protein in the cytoplasm, as determined by video-microscopy, Isoginkgetin and **IP2** did not triggered any changes in the fusion protein (Figures 5G and H). Similarly, even though MTX and OXA caused a nuclear decrease of the HMGB1-GFP fusion protein, isoginkgetin and **IP2** did not elicit any level changes of the fusion protein in the nuclear compartment of treated cells (Figures 5I and J). Altogether, these results demonstrate that the different spliceosome inhibitors, Isoginkgetin and **IP2** do not induce changes of the different parameters of ICD hallmarks at the chosen concentration and confirm that isoginkgetin and **IP2** are able to induce a specific immune response *in vivo* by only inhibiting the spliceosome without inducing ICD.

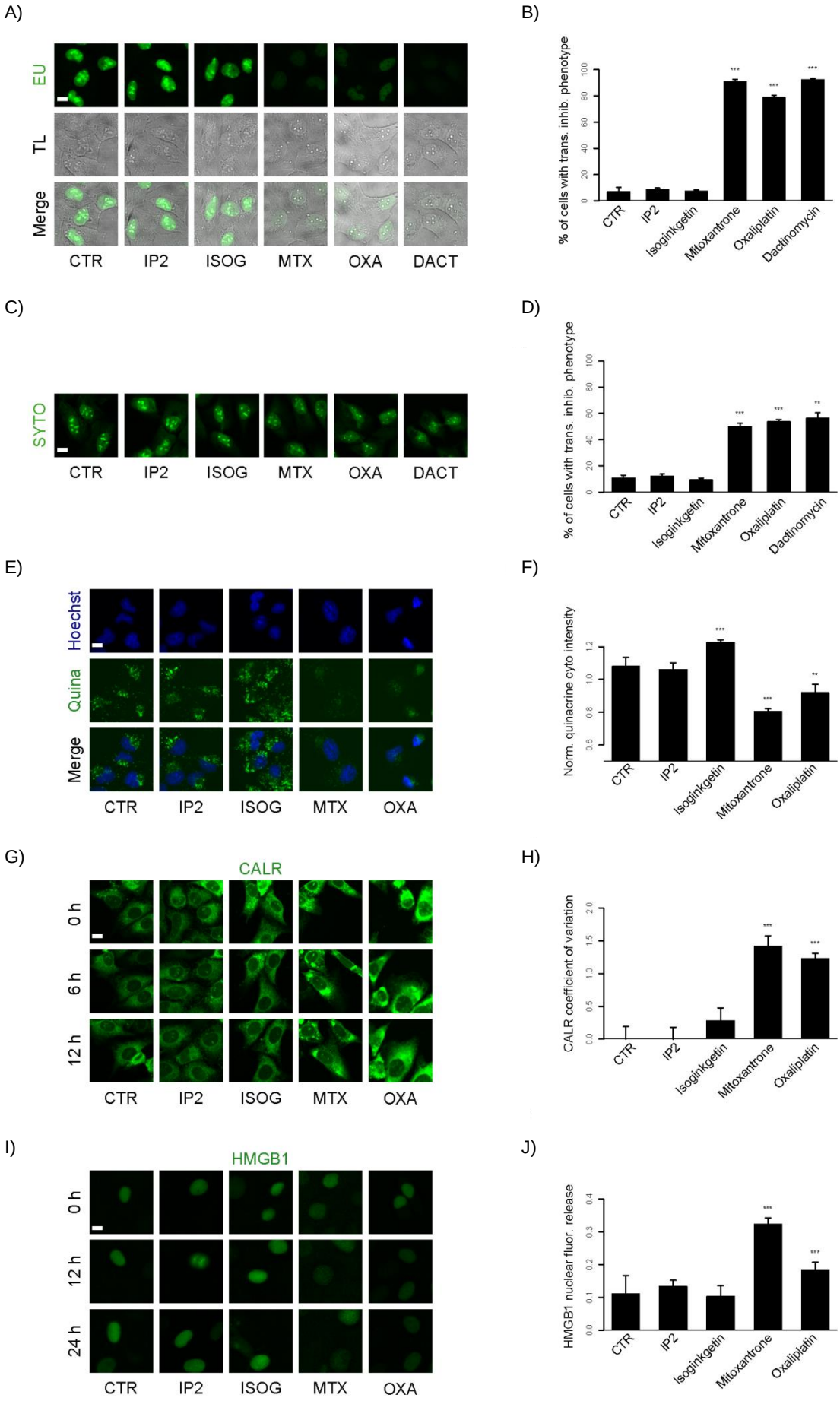
A)
EU
TL
Merge
CTR
IP2
ISOG
MTX
OXA
DACT
B)
% of cells with trans. inhib. phenotype
0
20
40
60
80
100
***
***
***
CTR
IP2
Isoginkgetin
Mitoxantrone
Oxaliplatin
Dactinomycin
C)
SYTO
CTR
IP2
ISOG
MTX
OXA
DACT
D)
% of cells with trans. inhib. phenotype
0
20
40
60
80
100
***
***
**
CTR
IP2
Isoginkgetin
Mitoxantrone
Oxaliplatin
Dactinomycin
E)
Hoechst
Quina
Merge
CTR
IP2
ISOG
MTX
OXA
F)
Norm. quinacrine cyto intensity
0.6
0.8
1.0
1.2
***
***
**
CTR
IP2
Isoginkgetin
Mitoxantrone
Oxaliplatin
G)
CALR
0 h
6 h
12 h
CTR
IP2
ISOG
MTX
OXA
H)
CALR coefficient of variation
0.0
0.5
1.0
1.5
2.0
***
***
CTR
IP2
Isoginkgetin
Mitoxantrone
Oxaliplatin
I)
HMGB1
0 h
12 h
24 h
CTR
IP2
ISOG
MTX
OXA
J)
HMGB1 nuclear fluor. release
0.0
0.1
0.2
0.3
0.4
***
***
CTR
IP2
Isoginkgetin
Mitoxantrone
Oxaliplatin

Figure 5. Isoginkgetin and IP2 do not induce immunogenic cell death hallmarks in human cancer cells *in vitro*. **(A-B)** Human osteosarcoma U2OS cells were left untreated (CTR) or pre-treated with 10 μM **IP2**, 10 μM isoginkgetin (ISOG), 3 μM mitoxantrone (MTX), 500 μM oxaliplatin (OXA) and 1 μM dactinomycin (DACT) for 2.5 h followed by an additional hour of treatment in the presence of 1 mM 5-ethynyl uridine (EU). Upon treatment, cells were fixed, permeabilized and EU was stained with an Alexa Fluor-488-coupled azide. **(A)** Representative images acquired by fluorescence and brightfield microscopy are shown for each treatment. **(B)** Cellular nuclei were automatically detected and classified by means of a pre-trained deep-learning model allowing to identify cells that undergo transcription inhibition. In the plot, the percentage of cells bearing a transcription inhibition phenotype is reported. **(C-D)** U2OS cells were left untreated (CTR) or treated with 10 μM **IP2**, 10 μM ISOG, 3 μM MTX, 500 μM OXA and 1 μM DACT for 4 h before fixation, RNA staining with SYTO RNASelect stain and image acquisition via fluorescence microscopy. **(C)** Representative images of each treatment are displayed. **(D)** The percentage of cells displaying a transcription inhibition phenotype was assessed using a pre-trained deep-learning model that detected and classify cellular nuclei encountering transcription inhibition. **(E-F)** U2OS cells were left untreated (CTR) or treated with 10 μM **IP2**, 10 μM ISOG, 3 μM MTX and 500 μM OXA for 24 h and ATP was stained with quinacrine. **(E)** Representative images acquired by live fluorescence microscopy are displayed for each condition. **(F)** The cytoplasmic green fluorescence intensity corresponding to the quinacrine signal was normalized to the untreated control (CTR) and values are reported in a bar chart. **(G-H)** U2OS cells stably expressing CALR-GFP and H2B-RFP or U2OS cells stably expressing HMGB1-GFP and H2B-RFP were left untreated (CTR) or treated with 10 μM **IP2**, 10 μM ISOG, 3 μM MTX and 500 μM OXA followed by immediate live cell acquisition with an image frequency of 1.5 h for 12 h and 24 h, respectively. **(H)** Representative time lapse images of CALR-GFP is depicted. **(I)** The area under curve (AUC) between 0 and 12 h of CALR intensity coefficient of variation is reported in a barchart. **(J)** For each cell, the relative nuclear fluorescence decrease calculated as the difference of HMGB1 nuclear green fluorescence intensity between two successive time points is depicted in a barchart. All scale bars equal 10 μm. For all barcharts, the mean ± SD of quadruplicates for one representative experiment is shown. Each value was compared to the control, and the *P*-value was calculated with pairwise Welch Student's *t*-test: *p<0.05, **p<0.01, ***p<0.001.

Intraperitoneal injection of IP2 is very well tolerated by C57BL/6 mice. After having shown that **IP2** can induce an immune response in vitro, that this activation is not due to phosphodiesterase inhibition or induction of immunogenic cell death, we wanted to define the maximum tolerated dose that can be used in vivo in order to avoid any negative endpoint associated with its administration, such as severe adverse behavior, weight loss>20% compared to pre-administration, or even death. Potential acute toxicity was assessed after a single intrapreritoneal (IP) injection of **IP2** at different concentrations to female C57BL/6 mice. No mortality was observed even at the maximum dose of 500 mg/kg.

No behavioral signs were observed immediately or after 30 minutes after IP2 injection at the injected doses. Furthermore, no notable clinical signs, such as weight loss of each mice treated (Figure 6) or organ damage (Suppl. Figure S2) were observed during the 15 days post-treatment compare to the PBS-treated animals. The only clinical sign that could be observed was a loss of kidney weight in mice treated at 250mg/kg only and not at a higher dose or lower dose (Table 4). From these results it can be concluded that the MTD level of IP2 formulated as a stable emulsion in sterile phosphate-buffered saline (PBS) after IP administration to female C57BL/6 mice is above 500 mg/kg.

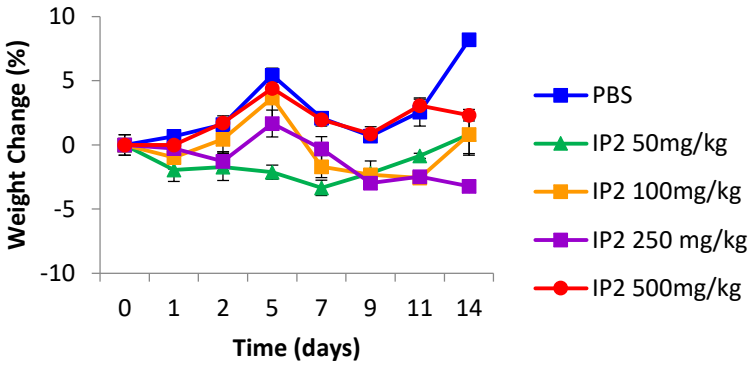

Figure 6: Animal body weight curves following IP2 treatment. Each mouse was intraperitoneally injected with the corresponding dose of IP2 and monitored for two weeks. Mice body weight was measured every 2 to 3 days.

Table 4: *Intraperitoneal injection of **IP2** is very well tolerated by C57BL/6 mice.* Each mouse was injected intraperitoneally with the corresponding dose of IP2 in a single dose and the weight of each cited organ was measured after 15 days of treatment.

		Mice weight	Leaver	Spleen	Kidneys
PBS	Mice n°1	24,2 g	1,3 g	0,1 g	0,3 g
	Mice n°2	23,5 g	1,2 g	0,2 g	0,3 g
IP2 50mg/kg	Mice n°3	19,5 g	1,0 g	0,1 g	0,3 g
	Mice n°4	22,5 g	1,1 g	0,2 g	0,3 g
IP2 100mg/kg	Mice n°5	22,7 g	1,0 g	0,1 g	0,2 g
	Mice n°6	19,5 g	1,0 g	0,1 g	0,3 g
IP2 250mg/kg	Mice n°7	19,1 g	0,9 g	0,1 g	0,1 g
	Mice n°8	20,0 g	1,0 g	0,1 g	0,1 g
IP2 500mg/kg	Mice n°9	20,4 g	1,2 g	0,1 g	0,2 g
	Mice n°10	21,3 g	1,0 g	0,1 g	0,2 g

IP2 induces tumor growth defects when injected intravenously. In a recent study[10], we demonstrated that **IP2** is capable of inducing a tumor growth defect in a fibrosarcoma model in vivo when injected intraperitoneally. In this new study, we wanted to evaluate the in vivo antitumor activity of **IP2** when injected by different routes such as intravenous and intratumoral. To this end, fibrosarcoma MCA205 WT cells were subcutaneously inoculated into C57BL/6 mice as previously described. From day 7 post cell inoculation and at day 12 and 17, each group of mice was intravenously treated with 2.5 mg/kg of **IP2**. At this dose, a significant decrease in MCA205 WT tumor growth over time was observed after treatment with **IP2** compare to the control group (Figures 7A and B). More specifically, we observed a 40% decrease in MCA205 WT fibrosarcoma growth at killing (Figure 7C) upon treatment with IP2 when injected intravenously.

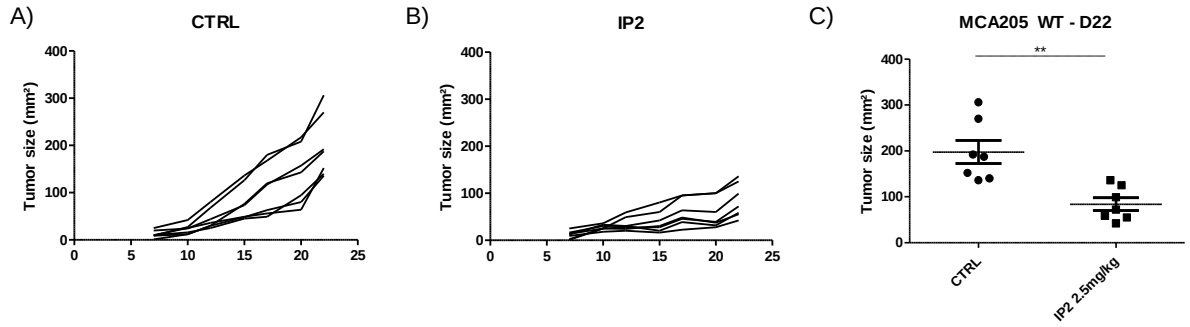

Figure 7: IP2 induces tumor growth defects when injected intravenously. A) and B) Individual tumor growth kinetics of MCA205 fibrosarcoma subcutaneously inoculated into the right flank of immunocompetent C57BL/6 mice previously treated with 2.5 mg/kg of **IP2** intravenously or not (control) from tumor cell inoculation. (C) Tumor size at killing of MCA205 fibrosarcoma subcutaneously inoculated into immunocompetent C57BL/6 mice previously treated with 2.5 mg/kg of **IP2** intravenously from tumor cell inoculation. **P < 0.01 (One way-ANOVA).

IP2 induces tumor growth defects when injected in an intratumoral ways. Moreover, in parallel to the previous experience with intravenous injection of IP2, we performed the same experience but this time by injecting IP2 intratumorally. For that purpose, fibrosarcoma MCA205 WT cells were subcutaneously inoculated into C57BL/6 mice as previously described. From day 7 post cell inoculation, each group of mice was intratumorally treated with 5 mg/kg of IP2 with three injections per week for two weeks. At this dose, a significant decrease in MCA205 WT tumor growth over time was observed after treatment with IP2 compare to the control group (Figures 8A and B). More precisely, we observed a 50% decrease in MCA205 WT fibrosarcoma growth at killing (Figure 8C) upon intratumoral treatment with IP2.

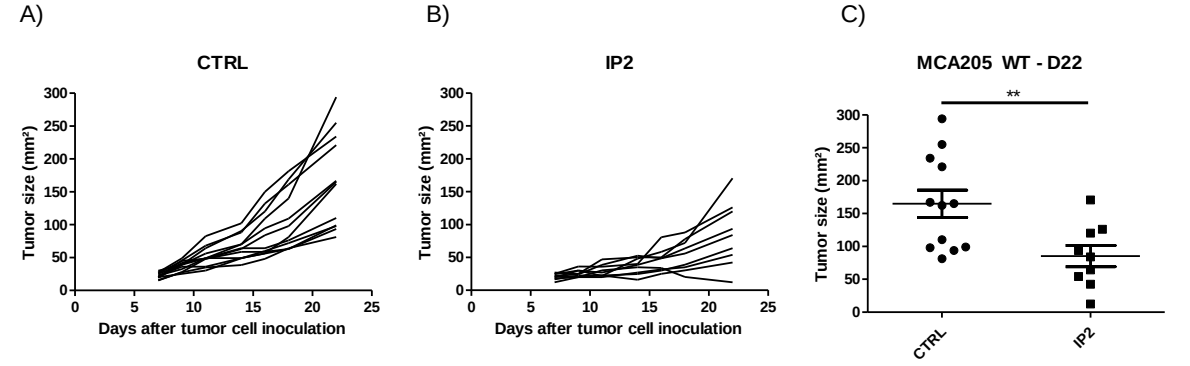

Figure 8: IP2 induces tumor growth defects when injected intratumorally. A) and B) Individual tumor growth kinetics of MCA205 fibrosarcoma subcutaneously inoculated into the right flank of immunocompetent C57BL/6 mice previously treated with 5 mg/kg of **IP2** intratumorally or not (control) from tumor cell inoculation. (C) Tumor size at killing of MCA205 fibrosarcoma subcutaneously inoculated into immunocompetent C57BL/6 mice previously treated with 5 mg/kg of **IP2** intratumorally from tumor cell inoculation. **P < 0.01 (One way-ANOVA).

In a recent study we demonstrated that **IP2** acts as an immunomodulatory agent *in vitro*, increasing PTP-derived antigen presentation in cancer cells. Furthermore, we demonstrate also that **IP2** is capable to impair tumor growth *in vivo* much more efficiently than isoginkgetin when injected in an intraperitoneal way. The result presented in this study so far

demonstrates that **IP2** has kept the capacity to induce tumor growth defect *in vivo* when **IP2** is injected in intravenous and intratumoral routes. Interestingly, in this study we demonstrate that **IP2** is stable in the plasma of mice but more surprisingly **IP2** bound at 98% to the plasma protein. From these results, it could have been concluded that **IP2** would not work when injected intravenously. Nevertheless, **IP2** induces tumor growth when injected intravenously.

It has been shown in various studies that human serum albumin (HSA) and alpha-1-acid glycoprotein (AAG) have a significant ability to bind to a wide variety of molecules serving as reservoirs for it.[22] As soon as **IP2** is injected intravenously, non-covalent interactions occur between the molecule and the different plasma proteins. In fact, we demonstrated that **IP2** interacts at 98% with plasma proteins. From this binding, we can speculate that we will have an important reservoir of **IP2** at the tumor site to reach its goal as a positive immunomodulator against tumor inducing a slowdown in tumor growth (Figures 3 and 4). These interactions and its intensity may vary according to the structural and physico-chemical properties of the molecule itself and the balance between the concentrations of the bound and free fractions of **IP2**.

Conclusion

In summary, we report for the first time the total synthesis of isoginkgetin natural product as well as the synthesis of three water soluble isoginkgetin-phosphates, the full study of the phosphate **IP2** from the point of view of its metabolic stability, pharmacokinetic as well as *in vitro* and *in vivo* biological activity. Although there is a need to better understand the effects of isoginkgetin and **IP2** on splicing inhibition, and given the fact that its compounds have a positive impact on anti-cancer immune responses, a broad field of studies on the link between splicing regulation and regulation of the MHC-I immunopeptidome is opening. Understanding these two phenomena will lead to the development of innovative anti-cancer immunotherapies targeting the splicing machinery.

EXPERIMENTAL SECTION

Materials and Instrumentation. Solvents and reagents are obtained from commercial suppliers and were used without further purification excepted with 2,4,6-trihydroxyactephenone monohydrate which was dried in an oven at 115°C overnight. For silica gel chromatography, the flash chromatography technique was used, with Merck silica gel 60 (230-400 mesh) and p.a. grade solvents unless otherwise noted. The ^{1}H NMR, ^{13}C NMR and ^{31}P NMR spectra were recorded in either $CDCl_3$, DMSO-d_6 or D_2O on Bruker Avance 300 spectrometers (^{1}H, 300 MHz; ^{13}C, 75 MHz; ^{31}P, 81 MHz). The chemical shifts of ^{1}H and ^{13}C are reported in ppm relative to the solvent residual peaks. Chemical shifts δ are given in ppm, and the following abbreviations are used: singlet (s), doublet (d), doublet of doublet (dd), triplet (t), quadruplet (q), and multiplet (m). High resolution mass spectra (HR-MS) were recorded on a MicroMass LCT Premier TOF ESI Spectrometer. The purity of the final compound **IP2** was determined to be ≥95% by means of analytical high pressure liquid chromatography−mass spectroscopy (HPLC− MS) on a Waters Alliance 2695 (HPLC) and LCT Premier, ESI-TOF (MS) system with an XBridge C18 column (2.1 × 150 mm, 3.5 µm) eluted at 0.25 mL/min with Milli-Q water + 0.1% formic acid/ CH_3CN, gradient 95/5 to 0/100 in 20 min. Reaction courses and product mixtures were routinely monitored by TLC on silica gel (precoated F254 Merck plates),

and compounds were visualized under a UVP Mineralight UVGL-58 lamp (254 nm) or by staining upon heating with vanillin solution (15 g of vanillin in 250 mL ethanol and 2.5 mL of concentrated sulfuric acid).

8-(5-(5,7-dimethoxy-4-oxo-4*H*-chromen-2-yl)-2-methoxyphenyl)-5,7-dimethoxy-2-(4-methoxyphenyl)-4*H*-chromen-4-one (1a)

Compound **1a** was prepared according to the following procedure: to a solution under argon of isoginkgetin (100 mg, 0.18 mmol, 1.0 equiv.) in anhydrous DMF (10 mL) were successively added K_2CO_3 (122 mg, 0.88 mmol, 5.0 equiv.) and iodomethane (83 µl, 1.33 mmol, 7 equiv.). The mixture was stirred at room temperature for 20 h and filtered. The solid was washed with water (3 x 30 mL) and the product was recovered by dissolution in a mixture DCM/MeOH (97/3). The solvents were evaporated under reduced pressure to yield **1a** as a beige solid (103 mg, 0.17 mmol, 94 %). **M.p.** = 177-179 °C. **^{1}H NMR** (300 MHz, $CDCl_3$) δ(ppm): 7.99 (dd, *J* = 8.6, 2 Hz, 1H), 7.96 (d, *J* = 2 Hz, 1H), 7.41 (d, *J* = 8.8 Hz, 2H), 7.17 (d, *J* = 8.7 Hz, 1H), 6.80 (d, *J* = 8.8 Hz, 2H), 6.66 (s, 1H), 6.61 (s, 1H), 6.56 (s, 1H), 6.52 (d, *J* = 2 Hz, 1H), 6.38 (d, *J* = 2 Hz, 1H), 4.09 (s, 3H), 3.96 (s, 3H), 3.92 (s, 3H), 3.86 (s, 3H), 3.79 (s, 3H), 3.77 (s, 3H). **^{13}C NMR** (75 MHz, $CDCl_3$) δ(ppm): 178.2, 177.8, 164.0, 162.1, 161.1, 161.1, 161.0, 160.8, 160.6, 160.3, 160.0, 156.3, 130.7, 127.6, 127.4, 123.8, 122.4, 114.4, 111.2, 108.0, 107.0, 106.8, 96.3, 93.0, 91.9, 56.6, 56.5, 56.3, 56.0, 55.8, 55.5. **HRMS** (ESI positive): calculated for $C_{36}H_{31}O_{10}$ $[M+H]^+$ 623.1912; found 623.1912.

5-hydroxy-8-(5-(5-hydroxy-7-methoxy-4-oxo-4*H*-chromen-2-yl)-2-methoxyphenyl)-7-methoxy-2-(4-methoxyphenyl)-4*H*-chromen-4-one (1b)

Compound **1b** was prepared according to the following procedure: to a solution of isoginkgetin (100 mg; 0.18 mmol; 1.0 equiv.) in anhydrous DMF (10 mL), was added K_2CO_3 (61 mg; 0.65 mmol; 2.5 equiv.) following by slow addition of iodomethane (22 µL; 0.35 mmol; 2 equiv.). The mixture was stirred at room temperature for 20 hours and the suspension was filtered and washed with ethyl acetate. The filtrate was washed 3 times with brine (3 x 30 mL) and the organic layer was dried over $MgSO_4$, filtered and condensed under reduced pressure. The resulting crude was purified by chromatography on a silica gel column (CH_2Cl_2/MeOH/HCl $1N_{(aq)}$: 99/1/0.1) to yield **1b** as a yellow powder (92 mg; 0.16 mmol; 88 %). **M. p.** = 289-291 °C. **^{1}H NMR** (300 MHz, $CDCl_3$) δ(ppm): 13.13 (s, 1H), 12.81 (s, 1H), 8.00 (dd, *J* = 8.6, 2 Hz, 1H), 7.98 (d, *J* = 2 Hz, 1H), 7.49 (d, *J* = 8.8 Hz, 2H), 7.18 (d, *J* = 8.7 Hz, 1H), 6.84 (d, *J* = 8.8 Hz, 2H), 6.63 (d, *J* = 9 Hz, 2H), 6.55 (s, 1H), 6.45 (d, *J* = 2 Hz, 1H), 6.38 (d, *J* = 2 Hz, 1H), 3.88 (s, 3H), 3.85 (s, 3H), 3.82 (s, 3H), 3.81 (s, 3H). **^{13}C NMR** (75 MHz, $CDCl_3$) δ(ppm): 182.9, 182.5, 165.6, 164.1, 163.9, 162.8, 162.7, 162.6, 162.3, 160.8, 157.9, 154.3, 131.2, 128.1, 127.8, 123.5, 122.2, 114.6, 111.3, 105.7, 105.2, 104.7, 103.7, 98.3, 95.5, 92.7, 56.4, 56.1, 55.9, 55.6. **HRMS** (ESI^+): calculated for $C_{34}H_{27}O_{10}$ $[M+H]^+$ 595.1599; found 595.1597.

7-hydroxy-8-(5-(7-hydroxy-5-methoxy-4-oxo-4*H*-chromen-2-yl)-2-methoxyphenyl)-5-methoxy-2-(4-methoxyphenyl)-4*H*-chromen-4-one (1c)

Step (a): To a solution of compound **1b** (105 mg, 0.18 mmol.) in THF (8 mL) was added NaH (60% in oil, 35 mg; 0.89 mmol; 5 equiv.), and stirred for 5 min at 20 °C. Then, diethylchlorophosphate (122 mg, 103 µl; 0.71 mmol, 4 equiv.) was added and the mixture was stirred at 20 °C for additional 30 min. 1 mL of H_2O was added to the reaction mixture and the solvent was concentrated under reduced pressure. Dichloromethane and water were added successively and after separation of the phases, the organic layer was collected and dried over $MgSO_4$, filtered and concentrated under reduced pressure. The crude product was purified by

chromatography on a silica gel column HCl_{1N}/MeOH/CH_2Cl_2 (0:0:100 to 0.1:2:98) and the desired diethylphosphate intermediate was isolated as a yellow powder (118 mg, 77% yield). ^{1}H NMR (300 MHz, $CDCl_3$, δ ppm):7.96 (dd, 1H, J_1 = 8.6Hz, J_2 = 1 Hz, ArH); 7.87 (d, 1H, *J* = 1Hz, ArH); 7.40 (d, 2H, *J* = 8.8 Hz, ArH); 7.18 (d, 2H, *J* = 5.6Hz, ArH); 6.97 (s, 1H, ArH); 6.79 (d, 2H, *J* = 8.8 Hz, ArH); 6.73 (s, 1H, ArH); 6.63 (s, 1H, ArH); 6.57 (s, 1H, ArH); 4.43 (m, 8H, *J* = 7 Hz, CH_2); 3.90 (s, 3H, OCH_3); 3.87 (s, 3H, OCH_3); 3.80 (s, 3H, OCH_3); 3.79 (s, 3H, OCH_3); 1.40 (m, 12H, *J* = 7Hz, CH_3). ^{13}C NMR (75 MHz, $CDCl_3$, δ en ppm): 176.9 (CO); 176.5 (CO); 163.2 (Ar); 162.2 (Ar); 161.2 (Ar); 160.4 (Ar); 160.1 (Ar); 158.9 (Ar); 155.4 (Ar); 150.4 (Ar); 130.4 (ArH); 127.9 (ArH); 127.4 (ArH); 123.5 (Ar); 123.4 (Ar); 121.8 (Ar); 114.4 (ArH); 111.5 (Ar); 111.2 (Ar); 111.2 (ArH); 107.5 (ArH); 106.3 (ArH); 106.2 (ArH); 102.0 (ArH); 98.0 (ArH); 65.1 ($2CH_2$); 56.4 (OCH_3); 56.0 (OCH_3); 55.9 (OCH_3); 55.4 (OCH_3); 16.1 ($2CH_3$). **HRMS** (ESI^+): calculated for $C_{42}H_{444}O_{16}P_2$ $[M+Na]^+$ 889,2002; found 889,2012.

Step (b): To a solution under argon of diethylphosphate intermediate (98 mg; 0.11 mmol; 1.0 equiv.) in anhydrous dichloromethane (8 mL) was added TMSI (0.905 mL; 0.905 mmol; 8.0 equiv.) and the reaction mixture was stirred at room temperature for 30 min. After evaporation of the solvent under reduced pressure, the yellow solid was dissolved in ethylacetate (5 mL), and evaporated under reduced pressure. Water then was added (2 mL) and evaporated under reduced pressure to yield the dihydrogen phosphate compound as a yellow solid (108 mg). ^{1}H NMR (300 MHz, DMSO-d_6, δ ppm): 8.25 (dd, 1H, J_1 = 8.9Hz, J_2 = 2 Hz, ArH); 8.06 (d, 1H, *J* = 2 Hz, ArH); 7.61 (d, 1H, *J* = 8.8 Hz, ArH); 7.51 (d, 1H, *J* = 8.7Hz, ArH); 7.39 (d, 1H, *J* = 8.8 Hz, ArH); 7.16 (d, 1H, *J* = 8.1 Hz, ArH); 6.90 à 6.84 (m+s, 6H, ArH); 3.84 (s, 3H, OCH_3); 3.83 (s, 3H, OCH_3);3.79 (s, 3H, OCH_3); 3.73 (s, 3H, OCH_3). ESI^+ $[M+H]^+$ calculated 595; found 595.

Step (c): To a suspension of dihydrogen phosphate compound in H_2O (2 mL) was added NaOH 1M (0.39 mL, 0.39 mmol; 4.0 equiv.). The solution was stirred at room temperature until a yellow solution was obtained. The solvent was evaporated under reduced pressure to yield **compound 1c** as a yellow solid (123 mg, quantitative yield). **^{1}H NMR** (300 MHz, D_2O) δ (ppm):7.53 - 6.18 (m, 12H, ArH); 3.67 (s, 3H, OCH_3); 3.53 (s, 3H, OCH_3); 3.52 (2s, 6H, OCH_3). **1c** is not ionised by ESI mass spectroscopy. **M.p.** > 350 °C. **HRMS** could not be determined due to the hydrolysis of phosphate during analysis.

Step (c): A suspension of dihydrogen phosphate compound in H_2O (2 mL) and NaOH 1M (0.39 mL, 0.39 mmol; 4.0 equiv.) was added. The solution was stirred at room temperature until to get a yellow solution. The solvent was evaporated under reduced pressure to yield **compound 1c** as a yellow solid (123 mg, quantitative yield). **^{1}H NMR** (300 MHz, D_2O) δ (ppm):7.53 - 6.18 (m, 12H, ArH); 3.67 (s, 3H, OCH_3); 3.53 (s, 3H, OCH_3); 3.52 (2s, 6H, OCH_3). **3c** is not ionised by ESI mass spectroscopy. **M.p.** > 350 °C. **HRMS** could not be determined due to the hydrolysis of phosphate during analysis.

8-(5-(7-((diethoxyphosphoryl)oxy)-5-hydroxy-4-oxo-4*H*-chromen-2-yl)-2-methoxyphenyl)-5-hydroxy-2-(4-methoxyphenyl)-4-oxo-4*H*-chromen-7-yl diethyl phosphate (2)

Compound **2** was prepared according to the following procedure: to a suspension under argon of isoginkgetin (561 mg, 0.99 mmol, 1.0 equiv.) in water (560 mL) was added KOH (445 mg, 7.92 mmol, 8.0 equiv.). The mixture was stirred at room temperature for 15 min, and were added successively dichloromethane (560 mL), tetrabutylammonium bromide (638 mg, 1.98 mmol, 2.0 equiv.) and diethylchlorophosphate (316 µl, 2.18 mmol, 2.2 equiv.). The reaction medium was stirred at room temperature for 2 h and after separation of the phases, the

organic layer was dried over $MgSO_4$, filtered and concentrated under reduced pressure. The crude product was purified by chromatography on a silica gel column (CH_2Cl_2/MeOH/HCl_{aq}(1N) :100:0:0 to 99:1:0.1) to yield **2** as a yellow powder (644 mg, 0.76 mmol, 77 %). **M.p.** = 154 - 156 °C. **^{1}H NMR** (300 MHz, $CDCl_3$) δ (ppm): 13.00 (s, 1H), 12.79 (s, 1H), 8.02 (dd, *J* = 8.7, 2.4 Hz, 1H), 7.97 (d, *J* = 2.4 Hz, 1H), 7.46 (d, *J* = 8.9 Hz, 2H), 7.18 (d, *J* = 8.8 Hz, 1H), 6.99 (s, 1H), 6.95 (s, 1H), 6.84 (d, *J* = 8.9 Hz, 2H), 6.65 (dd, *J* = 12.3, 5.1 Hz, 3H), 4.32 – 4.18 (m, 4H), 4.11 – 3.95 (m, 4H), 3.81 (m, 6H), 1.37 (t, *J* = 7.0 Hz, 6H), 1.22 (td, *J* = 6.7, 4.0 Hz, 6H). **^{13}C NMR** (75 MHz, $CDCl_3$) δ (ppm): 183.0, 182.7, 164.4, 162.9, 162.3, 161.9, 161.1, 157.1, 156.1, 156.0, 154.4, 153.6, 153.5, 131.2, 128.6, 127.9, 123.1, 123.1, 121.5, 114.7, 111.3, 108.3, 104.9, 104.3, 103.9, 103.9, 103.7, 99.1, 99.0, 65.2 (d, J = 6.0 Hz), 64.9 (d, J = 6.3 Hz), 56.1, 55.6, 16.3, 16.2, 16.1. **^{31}P NMR** (81 MHz, $CDCl_3$) δ: -7.32, -7.53. **HRMS** (ESI^+): calculated for $C_{40}H_{41}O_{16}P_2$ $[M+H]^+$ 839.1864; found 839.1865.

8-(5-(7-((diethoxyphosphoryl)oxy)-5-methoxy-4-oxo-4*H*-chromen-2-yl)-2-methoxyphenyl)-5-methoxy-2-(4-methoxyphenyl)-4-oxo-4*H*-chromen-7-yl diethyl phosphate (3)

Compound **3** was prepared according to the following procedure: to a solution under argon of **2** (109 mg; 0.13 mmol; 1.0 equiv.) in anhydrous DMF (1.5 mL) were successively added K_2CO_3 (90 mg, 0.65 mmol, 5.0 equiv.) and iodomethane (24 µl, 0.39 mmol, 3.0 equiv.). The mixture was stirred at room temperature for 20 h and filtered. The solid was washed with ethyl acetate and the filtrate was washed with brine (3 x 30 mL). The organic layer was dried over $MgSO_4$, filtered and concentrated under reduced pressure to yield **3** as a yellow powder (109 mg, 0.13 mmol, 97 %). **M. p.** = 141-143 °C. **^{1}H NMR** (300 MHz, $CDCl_3$) δ (ppm): 7.99 (dd, *J* = 8.8, 2.1 Hz, 1H), 7.93 (d, *J* = 2.2 Hz, 1H), 7.38 (d, *J* = 8.9 Hz, 2H), 7.16 (d, J = 8.7 Hz, 1H), 7.11 (s, 1H), 7.04 (s, 1H), 6.80 (d, *J* = 8.9 Hz, 2H), 6.67 (m, 3H), 4.31 – 4.18 (m, 4H), 4.16 – 3.90 (m, 10H), 3.78 (d, *J* = 3.3 Hz, 6H), 1.36 (t, *J* = 7.1 Hz, 6H), 1.22 (m, 6H). **^{13}C NMR** (75 MHz, $CDCl_3$) δ: 177.9, 177.4, 162.3, 161.2, 161.0, 160.9, 160.5, 160.4, 158.9, 156.4, 154.8, 154.8, 152.3, 152.2, 130.7, 128.1, 127.5 (2C), 123.4, 123.3, 121.6, 114.5 (2C), 112.0, 111.1, 108.0, 107.3, 101.1, 101.1, 99.9, 99.8, 99.5, 65.2 (d, *J* = 6.3 Hz, 2C), 65.1 (d, J = 6.4 Hz), 64.9 (d, J = 6.6 Hz), 56.9, 56.8, 56.0, 55.5, 16.3, 16.2, 16.1, 16.0. **^{31}P NMR** (81 MHz, $CDCl_3$) δ: -7.17, -7.80. **HRMS** (ESI^+): calculated for $C_{42}H_{45}O_{16}P_2$ $[M+H]^+$ 867.2177; found 867.2182.

Sodium 5-methoxy-8-(2-methoxy-5-(5-methoxy-4-oxo-7-(phosphonatooxy)-4*H*-chromen-2-yl)phenyl)-2-(4-methoxyphenyl)-4-oxo-4*H*-chromen-7-yl phosphate (M2P2)

Compound **M2P2** was prepared according to the following procedure: to a solution under argon of **2** (109 mg; 0.13 mmol; 1.0 equiv.) in anhydrous dichloromethane (8 mL) was added TMSBr (5.2 mmol; 40 equiv.) and the reaction mixture was stirred at room temperature for 16 hours. After evaporation of the solvent under reduced pressure, the yellow solid was dissolved in anhydrous methanol (4 mL) and NaOH (21 mg; 0.52 mmol; 4.0 equiv.) was added. The solution was stirred at room temperature for 30 min and the solvent was evaporated under reduced pressure to yield **M2P2** as a yellow solid (101 mg, 0.12 mmol, 95 %). **M. p.** >350 °C. **^{1}H NMR** (300 MHz, D_2O) δ(ppm): 7.81 (s, 1H), 7.71 (m, 1H), 7.41 (s, 1H), 7.23 – 6.93 (m, 4H), 6.81 (s, 1H), 6.54 (m, 3H), 6.33 (s, 1H), 4.05 (s, 3H), 3.94 (s, 3H), 3.70 (s, 3H), 3.54 (s, 3H). **^{13}C NMR** (75 MHz, D_2O) δ(ppm): 179.9, 162.4, 161.5, 160.8, 160.4, 160.3, 160.2, 160.1, 159.9,

159.7, 159.4, 158.9, 157.9, 155.6, 130.9, 128.1, 127.1, 126.7, 122.8, 122.1, 113.8, 111.6, 108.2, 107.6, 105.9, 104.9, 100.9, 99.6, 56.3, 56.2, 56.2, 56.0. **^{31}P NMR** (81 MHz, $CDCl_3$) δ (ppm): -0.16, -0.80. **HRMS** could not be determined due to the hydrolysis of phosphate during analysis.

Sodium 5-hydroxy-8-(5-(5-hydroxy-4-oxo-7-(phosphonatooxy)-4*H*-chromen-2-yl)-2-methoxyphenyl)-2-(4-methoxyphenyl)-4-oxo-4*H*-chromen-7-yl phosphate (IP2)

Compound **IP2** was prepared according to the following procedure: to a solution under argon of **2** (1.5 g; 1.82 mmol; 1.0 equiv.) in anhydrous dichloromethane (36 mL) was added TMSBr (9.6 mL; 72.8 mmol; 40.0 equiv.) and the reaction mixture was stirred at room temperature for 16 hours. After evaporation of the solvent under reduced pressure, the yellow solid (2.1 g) was dissolved in anhydrous methanol (60 mL) and NaOH (291 mg; 7.28 mmol; 4.0 equiv.) was added. The solution was stirred at room temperature for 30 min and the solvent was evaporated under reduced pressure to yield **IP2** as a yellow solid (1.4 g; 1.74 mmol; 96 %). **M. p.** >350 °C. **^{1}H NMR** (300 MHz, D_2O) δ(ppm): 7.64 (brs, 1H), 7.51 (brs, 1H), 7.24 (s, 1H), 7.00 (brs, 3H), 6.81 (d, *J* = 7.0 Hz, 2H), 6.58 – 6.41 (m, 3H), 6.33 (brs, 1H), 3.83 (s, 3H), 3.63 (s, 3H). **^{13}C NMR** (75 MHz, D_2O) δ(ppm): 182.5, 164.5, 161.8, 160.9, 160.8, 160.4, 159.4, 159.3, 158.6, 156.9, 153.7, 130.9, 128.3, 127.3 (2C), 122.5, 122.1, 121.5, 114.0 (2C), 111.8, 107.2, 107.1, 105.5, 104.9, 103.6, 103.3, 102.6, 99.8, 99.7, 56.1, 55.4. **^{31}P NMR** (81 MHz, D_2O) δ: -0.49, -1.59. **HRMS** (ESI^-): calculated for $C_{32}H_{23}O_{16}P_2$ $[M-H]^-$ 725.0467; found 725.0466.

Acacetin or 5,7-dihydroxy-2-(4-methoxyphenyl)-4*H*-chromen-4-one (4)

Compound **4** was prepared according to the following procedure[23]: to a suspension under argon of phloroglucinol (1.0 g ; 7.93 mmol ; 1.0 equiv.) in ethyl 4-methoxybenzoylacetate (2.7 mL ; 12.69 mmol ; 1.6 equiv.) in a round bottom flask bearing a distillation apparatus was added DMAP (73 mg ; 0.55 mmol ; 0.08 equiv.). The suspension was stirred at room temperature for 5 minutes and gradually heated at 200°C (from room temperature to 200 °C in about 15 min). After 3h at 200°C, the mixture was allowed to being cooled at room temperature. The product was suspended in ethyl acetate, washed with ethyl acetate and dry to yield **4** as a beige powder (990 mg; 3.48 mmol ; 44 %). **M.p.**: 252-254°C. **^{1}H NMR** (300 MHz, DMSO-d_6) δ (ppm): 12.92 (s, 1H), 10.72 (s, 1H), 8.02 (d, J = 8.3 Hz, 2H), 7.11 (d, *J* = 8.4 Hz, 2H), 6.85 (s, 1H), 6.50 (d, *J* = 2.0 Hz, 1H), 6.20 (d, *J* = 2.0 Hz, 1H), 3.86 (s, 3H). **^{13}C NMR** (75 MHz, DMSO-d_6) δ (ppm): 181.7, 164.2, 163.2, 162.2, 161.4, 157.3, 128.2, 122.8, 114.5, 103.7, 103.5, 98.8, 94.0, 55.5. **HRMS** (ESI^+): calculated for $C_{16}H_{13}O_5$ $[M+H]^+$ 285.0757; Found 285.0759.

5,7-bis(benzyloxy)-2-(4-methoxyphenyl)-4*H*-chromen-4-one (5)

Compound **5** was prepared according to the following procedure: to a solution under argon of **4** (5.8 g ; 20.42 mmol ; 1.0 equiv.) in DMF (68 mL) were added K_2CO_3 (8.4 g ; 61.26 mmol ; 2.7 equiv.) and BnBr (7.2 mL ; 61.26 mmol ; 2.7 equiv.). The mixture was stirred at room temperature for 16 h and heated at 50°C for 8h. After cooling to room temperature, water (600 mL) was added and the resulting precipitate was recovered by filtration and dry. The resulting crude was purified by chromatography on a silica gel column (cyclohexane/ethyl acetate : 8/2 to 0/1) to yield **5** as a beige powder (5.7 g ; 12.25 mmol ; 60 %). **M.p.**: 164-166°C. **^{1}H NMR** (300 MHz, $CDCl_3$) δ (ppm): 7.73 (d, *J* = 9.0 Hz, 2H), 7.50 (d, *J* = 7.3 Hz, 2H), 7.38 – 7.25 (m, 6H), 7.25 – 7.10 (m, 2H), 6.90 (d, *J* = 9.0 Hz, 2H), 6.65 (s, 1H), 6.56 (d, *J* = 2.3 Hz, 1H), 6.40 (d, *J* = 2.4 Hz, 1H), 5.13 (s, 2H), 5.02 (s, 2H), 3.77 (s, 3H). **^{13}C NMR** (75 MHz, $CDCl_3$) δ (ppm):

177.5, 163.1, 162.3, 161.1, 159.9, 136.6, 135.9, 128.9, 128.7, 128.6, 127.9, 127.8, 127.7, 126.8, 124.0, 114.5, 109.9, 107.7, 102.0, 98.6, 94.5, 55.6. **HRMS** (ESI^+): calculated for $C_{30}H_{24}NaNO_5$ $[M+Na]^+$ 487.1516; Found 487.1520.

5,7-bis(benzyloxy)-8-iodo-2-(4-methoxyphenyl)-4*H*-chromen-4-one (6)

Compound **6** was prepared according to the following procedure[24] : to a solution under argon and cooled at 0°C of **5** (2.0 g ; 4.31 mmol ; 1.0 equiv.) in dry DCM (21 mL) were added I_2 (1.1 g ; 4.52 mmol ; 1.05 equiv.) and AgOTf (1.3 g ; 5.17 mmol ; 1.2 equiv.). The mixture was stirred at 0°C for 2h and I_2 (550 mg ; 2.25 mmol ;0.52 equiv.) and AgOTf (650 mg ; 2.6 mmol ; 0.60 equiv.) were added. The mixture was stirred at 0°C for 1.5h and then diluted with acetone (200 mL). The suspension was filtered on a celite pad and washed with acetone. The filtrate was condensed under reduced pressure and the crude was purified by chromatography on a silica gel column (DCM/MeOH: 1/0 to 99.4/0.6) to yield **6** as a pale yellow powder (1.6 g ; 2.67 mmol; 62 %). **M.p.**: 202-204°C. **^{1}H NMR** (300 MHz, $CDCl_3$) δ (ppm): 8.01 (d, *J* = 9.0 Hz, 2H), 7.60 – 7.52 (m, 2H), 7.48 – 7.28 (m, 8H), 7.03 (d, *J* = 9.0 Hz, 2H), 6.62 (s, 1H), 6.47 (s, 1H), 5.23 (s, 2H), 5.18 (s, 2H), 3.89 (s,3H). **^{13}C NMR** (75 MHz, $CDCl_3$) δ (ppm) : 177.3, 162.5, 161.5, 161.4, 160.6, 136.3, 135.7, 128.9, 128.8, 128.4, 128.4, 128.0, 127.2, 126.9, 123.7, 114.6, 107.1, 96.3, 71.5, 71.5, 55.6. **HRMS** (ESI^+): calculated for $C_{30}H_{23}INaO_5$ $[M+Na]^+$ 613.0482; Found 613.0487.

1-(2-hydroxy-4,6-bis(methoxymethoxy)phenyl)ethan-1-one (7)

Compound **7** was prepared according to the following procedure[25]: to a suspension under argon and cooled at 0°C of 2,4,6-trihydroxyacetophenone (8.0 g ; 47.58 mmol ; 1 equiv.) in anhydrous DCM (80 mL) was added DIPEA (17.0 mL ; 99.92 mmol ; 2.1 equiv.). The mixture was stirred at 0°C for 15min and was added dropwise and at 0°C MOMCl (7.8 mL ; 99.92 mmol ; 2.1 equiv.). The mixture was stirred at room temperature for 45min and was poured on water. The product was extracted with DCM and the combined organic layers were washed with brine, dried over $MgSO_4$, filtered and condensed under reduced pressure. The resulting crude was purified by chromatography on a silica gel column (cyclohexane/ethyl acetate : 9/1) to yield **7** as a white solid (7.8 g ; 30.45 mmol ; 64 %). **M.p.**: 51-53°C. **^{1}H NMR** (300 MHz, $CDCl_3$) δ (ppm): 13.69 (s, 1H), 6.24 (t, *J* = 2.5 Hz, 2H), 5.25 (s, 2H), 5.17 (s, 2H), 3.52 (s, 3H), 3.47 (s, 3H), 2.65 (s, 3H). **^{13}C NMR** (75 MHz, CDCl3) δ (ppm): 203.3, 166.9, 163.6, 160.5, 107.1, 97.3, 94.6, 94.2, 56.8, 56.5, 33.0. **HRMS** (ESI^+): calculated for $C_{12}H_{16}NaO_6$ $[M+Na]^+$ 279.0839; Found 279.0839.

1-(2-(benzyloxy)-4,6-bis(methoxymethoxy)phenyl)ethan-1-one (8)

Compound **8** was prepared according to the following procedure[25]: to a solution under argon of **7** (4.0 g ; 15.6 mmol ; 1.0 equiv.) in anhydrous DMF (24 mL) were added K_2CO_3 (3.2 g ; 23.40 mmol ; 1.5 equiv.) and BnCl (2.15 mL ; 23.40 mmol ; 1.2 equiv.). The mixture was heated at 80°C for 5 hours and was allowed to being cool to room temperature. The suspension was poured onto water (400 mL) and the product was extracted with DCM. The combined organic layers were washed with brine, dried over MgSO4, filtered and condensed under reduced pressure. The resulting crude was purified by chromatography on a silica gel column (cyclohexane/ethyl acetate : 5/1) to yield **8** as a white powder (4.5 g ; 12.95 mmol ; 83 %). **M.p.**: 64-66°C. **^{1}H NMR** (300 MHz, $CDCl_3$) δ (ppm): 7.36 (m, 5H), 6.46 (s, 1H), 6.38 (d, *J* = 1.9 Hz, 1H), 5.13 (s, 4H), 5.06 (s, 2H), 3.46 (s, 6H), 2.48 (s, 3H). **^{13}C NMR** (75 MHz, $CDCl_3$) δ (ppm): 201.5, 159.7, 157.0, 155.5, 136.5, 128.7, 128.1, 127.4, 116.7, 96.7, 95.6, 95.0, 94.7, 70.7, 56.5, 56.3, 32.7. **HRMS** (ESI^+): calculated for $C_{19}H_{23}O_6$ $[M+H]^+$ 347.1489; Found 347.1495.

1-(2-(benzyloxy)-4,6-dihydroxyphenyl)ethan-1-one (9)

Compound **9** was prepared according to the following procedure[25]: to a suspension of **8** (18.4 g; 53.12 mmol ; 1.0 equiv.) in MeOH (350 mL) was added a aqueous solution of HCl 2N (53 mL). The mixture was refluxed for 1 hour and was allowed to being cooled to room temperature. The product was recovered by filtration, washed with water and dried to yield **9** as a white solid (11.6 g ; 44.91 mmol ; 84 %). **M.p.**: 239-241°C. **^{1}H NMR** (300 MHz, DMSO-d_6) δ (ppm): 10.59 (s, 1H), 7.54 – 7.46 (m, 2H), 7.46 – 7.27 (m, 3H), 6.08 (d, *J* = 2.2 Hz, 1H), 5.91 (d, *J* = 2.2 Hz, 1H), 5.14 (s, 2H), 2.47 (s, 3H). **^{13}C NMR** (75 MHz, DMSO-d_6) δ (ppm): 202.1, 166.3, 164.9, 162.2, 136.0, 128.4, 128.0, 104.8, 95.8, 92.4, 70.4, 32.7. **HRMS** (ESI$^+$): calculated for $C_{15}H_{15}O_4$ $[M+H]^+$ 259.0965; Found 259.0969.

1-(2,4-bis(benzyloxy)-6-hydroxyphenyl)ethan-1-one (10)

Compound **10** was prepared according to the following procedure[25]: to a solution under argon and cooled at 0°C of **9** (11.6 g ; 44.91 mmol ; 1.0 equiv.) in anhydrous DMF (112 mL) was added K_2CO_3 (6.5 g ; 47.15 mmol ; 1.05 equiv.) and BnCl (5.4 mL ; 47.15 mmol ; 1.05 equiv.). After stirring at 0°C for 10min, the mixture was stirred at room temperature for 16 hours. The mixture was poured on an aqueous solution of HCl 1N and the product was extracted with ethyl acetate. The combined organic layers were washed with brine, dried over $MgSO_4$, filtered and condensed under reduced pressure. The resulting crude was purified by chromatography on a silica gel column (cyclohexane/ethyl acetae : 9/1) to yield **10** as a white solid (11.7 g ; 33.57 mmol ; 75 %). **M.p.**: 109-111°C. **^{1}H NMR** (300 MHz, $CDCl_3$) δ (ppm): 14.01 (s, 1H), 7.56 – 7.31 (m, 10H), 6.19 (d, *J* = 2.4 Hz, 1H), 6.12 (d, *J* = 2.4 Hz, 1H), 5.09 (s, 2H), 5.08 (s, 2H), 2.57 (s, 3H). **^{13}C NMR** (75 MHz, $CDCl_3$) δ (ppm): 203.3, 167.7, 165.3, 162.2, 136.1, 135.8, 128.9, 128.9, 128.6, 128.5, 128.1, 127.8, 95.0, 92.5, 71.3, 70.4, 33.4. **HRMS** (ESI+): calculated for $C_{22}H_{21}O_4$ $[M+H]^+$ 349.1434; Found 349.1434.

3-iodo-4-methoxybenzaldehyde (11)

Compound **11** was prepared according to the following procedure[26]: to a solution *p*-anisaldéhyde (5 mL ; 37.29 mmol ; 1 equiv.) in glacial acetic acid (50 mL) heated at 60°C was added a solution of ICl (5.96 g ; 37.29 mmol ; 2 equiv.) in DCM (37 mL). The mixture was heated at 80°C for 24 hours and was allowed to being cooled to room temperature. An aqueous solution of $Na_2S_2O_4$ was added until decoloration of the solution and DCM was evaporated under reduced pressure. The mixture was cooled at 0°C in an ice bath and the white precipitate was collected by filtration and washed with methanol to yield **11** as a solid (7.7 g ; 29.36 mmol ; 79 %). **M.p.**: 107-109°C. **^{1}H NMR** (300 MHz, $CDCl_3$) δ (ppm): 9.82 (s, 1H), 8.30 (d, *J* = 2.1 Hz, 1H), 7.85 (dt, *J* = 8.7, 2.4 Hz, 1H), 6.92 (d, *J* = 8.5 Hz, 1H), 3.97 (s, 3H). **^{13}C NMR** (75 MHz, $CDCl_3$) δ (ppm): 189.4, 162.9, 141.2, 132.2, 131.6, 110.7, 86.6, 56.9. **HRMS** (ESI$^+$): calculated for $C_8H_8IO_2$ $[M+H]^+$ 262.9563; Found 262.9570.

(E)-1-(2,4-bis(benzyloxy)-6-hydroxyphenyl)-3-(3-iodo-4-methoxyphenyl)prop-2-en-1-one (12)

Compound **12** was prepared according to the following procedure[24]: to a solution under argon and cooled at 0°C of **10** (1.3 g; 3.73 mmol ; 1 equiv.) in anhydrous DMF (5 mL) was added NaH 60% in mineral oil (182 mg ; 4.56 mmol ; 1.2 equiv.). The mixture was stirred at 0°C for 20 min and a solution of **11** (1.0 g; 3.8 mmol) in anhydrous DMF (3 mL) was added dropwise and at 0°C. The red mixture was stirred at room temperature for 16h and acidified to pH 2 with an aqueous solution of HCl 1N.The resulting yellow precipitate was recovered by filtration,

washed with water then methanol to yield **12** as a yellow solid (1.0 g ; 1.69 mmol ; 46 %). **M.p.**: 164-166°C. **^{1}H NMR** (300 MHz, $CDCl_3$) δ (ppm): 14.38 (s, 1H), 7.77 – 7.68 (m, 2H), 7.59 (d, *J* = 15.5 Hz, 1H), 7.55 – 7.33 (m, 10H), 7.03 (dd, *J* = 8.6, 2.2 Hz, 1H), 6.61 (d, *J* = 8.6 Hz, 1H), 6.22 (d, *J* = 2.4 Hz, 1H), 6.17 (d, *J* = 2.4 Hz, 1H), 5.10 (s, 2H), 5.07 (s, 2H), 3.90 (s, 3H). **^{13}C NMR** (75 MHz, $CDCl_3$) δ (ppm): 192.5, 168.6, 165.4, 161.8, 159.5, 140.9, 139.8, 129.9, 129.1, 128.9, 128.8, 128.5, 128.4, 127.8, 126.6, 110.8, 106.7, 95.3, 92.9, 86.4, 71.5, 70.5, 56.6. **HRMS** (ESI^+): calculated for $C_{30}H_{26}IO_5$ $[M+H]^+$ 593.0819; Found 593.0828.

5,7-bis(benzyloxy)-2-(3-iodo-4-methoxyphenyl)-4*H*-chromen-4-one (13)

Compound **13** was prepared according to the following procedure[24]: to a solution under argon of **12** (970 mg; 1.64 mmol; 1.0 equiv.) in anhydrous DMSO (3 mL) was added iodine (21 mg; 0.08 mmol ; 0.05 equiv.). The mixture was heated at 100°C for 16h and was allowed to being cooled to room temperature. A saturated aqueous solution of $Na_2S_2O_3$ was added until decoloration of the solution. The resulting precipitate was collected by filtration and washed with a few of methanol. The resulting crude was purified by chromatography on a silica gel column (cyclohexane/ethyl acetate : 5/5) to yield **13** as pale yellow solid (880 mg ; 1.49 mmol ; 93 %). **M.p.**: 215-217°C. **^{1}H NMR** (300 MHz, $CDCl_3$) δ (ppm): 8.30 (d, *J* = 2.0 Hz, 1H), 7.81 (dd, *J* = 8.7, 2.0 Hz, 1H), 7.66 – 7.58 (m, 2H), 7.52 – 7.36 (m, 7H), 7.32 (d, *J* = 7.4 Hz, 1H), 6.90 (d, *J* = 8.6 Hz, 1H), 6.68 (d, *J* = 2.1 Hz, 1H), 6.56 (s, 1H), 6.51 (d, *J* = 2.0 Hz, 1H), 5.24 (s, 2H), 5.14 (s, 2H), 3.96 (s, 3H). **^{13}C NMR** (75 MHz, $CDCl_3$) δ (ppm): 177.2, 163.1, 160.5, 159.9, 159.2, 137.2, 136.5, 135.8, 128.9, 128.7, 128.6, 127.8, 127.6, 126.7, 125.9, 110.9, 110.0, 108.4, 98.7, 94.4, 86.5, 70.9, 70.7, 56.7. **HRMS** (ESI^+): calculated for $C_{30}H_{23}INaO_5$ $[M+Na]^+$ 613.0482; Found 613.0484.

5,7-bis(benzyloxy)-2-(4-methoxy-3-(4,4,5,5-tetramethyl-1,3,2-dioxaborolan-2-yl)phenyl)-4*H*-chromen-4-one (14)

Compound **14** was prepared according to the following procedur[27]: in a microwave reactor under argon were added **13** (548 mg ; 0.93 mmol ; 1.0 equiv.), $PdCl_2$(dppf) (34 mg ; 0.05 mmol ; 0.05 equiv.), bis(pinacolato)diboron (307 mg ; 1.21 mmol ; 1.3 equiv.) and potassium acetate (364 mg ; 3.72 mmol ; 4.0 equiv.). The reactor was sealed, purged with argon and was added anhydrous DMF (10 mL). The mixture was heated at 80°C for 5 hours and was allowed to being cooled to room temperature. The mixture was diluted with an aqueous solution of HCl 1N and the product was extracted with ethyl acetate. The combined organic layers were washed with brine, dried over $MgSO_4$, filtered and condensed under reduced pressure. The resulting crude was purified by chromatography on a silica gel column (cyclohexane/ethyl acetate : 5/5) to yield **14** as a white solid (257 mg ; 0.44 mmol ; 47 %). **M.p.**: 159-161°C. **^{1}H NMR** (300 MHz, $CDCl_3$) δ (ppm): 8.17 (s, 1H), 7.91 (d, *J* = 8.0 Hz, 1H), 7.62 (d, *J* = 7.6 Hz, 2H), 7.41 (m, 8H), 6.96 (d, *J* = 9.0 Hz, 1H), 6.69 (s, 1H), 6.63 (s, 1H),6.50 (s, 1H), 5.25 (s, 2H), 5.12 (s, 2H), 3.91 (s, 3H), 1.39 (s, 12H). **^{13}C NMR** (75 MHz, $CDCl_3$) δ (ppm): 177.5, 166.6, 162.9, 161.0, 159.9, 159.9, 136.7, 136.0, 134.9, 130.5, 128.9, 128.7, 128.6, 127.8, 127.7, 126.8, 123.5, 110.7, 108.1, 98.6, 94.7, 84.1, 71.0, 70.7, 56.1, 25.0. **HRMS** (ESI^+): calculated for $C_{36}H_{35}BNaO_7$ $[M+Na]^+$ 613.2368; Found 613.2381.

5,7-bis(benzyloxy)-8-(5-(5,7-bis(benzyloxy)-4-oxo-4*H*-chromen-2-yl)-2-methoxyphenyl)-2-(4-methoxyphenyl)-4*H*-chromen-4-one (15)

Compound **15** was prepared according to the following procedure[27]: in a microwave reactor under argon were added **14** (250 mg ; 0.42 mmol ; 1.0 equiv.), **6** (250 mg ; 0.42 mmol ; 1.0

equiv.), $Pd(PPh_3)_4$ (24 mg ; 0.02 mmol ; 0.05 equiv.) and NaOH (67 mg ; 1.68 mmol). The reactor was sealed, purged with argon and was added a mixture of DMF/H_2O (10 mL ; 9/1). The mixture was heated at 80°C for 5 hours and was allowed to being cooled to room temperature. The mixture was filtered on a celite pad and washed with a mixture of DCM and methanol. An aqueous solution of HCl 1N was added to the filtrate and the product was extracted with ethyl acetate. The combined organic layers were washed with brine, dried over $MgSO_4$, filtered and condensed under reduced pressure. The resulting crude was purified by chromatography on a silica gel column (cyclohexane/ethyl acetate : 5/5) to yield **15** as a white solid (250 mg ; 0.17 mmol ; 40 %). **M.p.**: 251-253°C. **^{1}H NMR** (300 MHz, DMSO-d_6) δ (ppm): 8.14 (dd, J = 8.7, 2.4 Hz, 1H), 8.09 (d, J = 2.4 Hz, 1H), 7.72 – 7.66 (m, 2H), 7.66 – 7.59 (m, 3H), 7.53 (d, *J* = 8.9 Hz, 2H), 7.39 (m, 14H), 7.25 (dd, *J* = 5.0, 2.1 Hz, 2H), 7.04 (s, 1H), 6.99 (d, *J* = 2.2 Hz, 1H), 6.89 (d, *J* = 9.0 Hz, 2H), 6.74 (s, 1H), 6.70 (d, *J* = 2.3 Hz, 1H), 6.67 (s, 1H), 5.37 (s, 2H), 5.30 (d, *J* = 7.4 Hz, 2H), 5.23 (s, 2H), 5.18 (s, 2H), 3.75 (s, 3H), 3.73 (s, 3H). **^{13}C NMR** (75 MHz, DMSO-d_6) δ (ppm): 175.9, 175.5, 162.5, 161.6, 159.7, 159.7, 159.5, 159.1, 158.9, 158.9, 155.4, 136.9, 136.8, 136.3, 136.0, 131.9, 131.5, 131.3, 130.4, 128.6, 128.4, 128.3, 128.2, 128.1, 127.9, 127.5, 127.3, 127.2, 126.9, 126.7, 123.0, 122.6, 121.6, 114.3, 111.5, 108.8, 108.5, 107.2, 107.0, 106.2, 98.2, 95.8, 94.6, 70.1, 70.1, 69.9, 69.9, 55.7, 55.3. **HRMS** (ESI^+): calculated for $C_{60}H_{47}O_{10}$ $[M+H]^+$ 927.3164; Found 927.3164.

8-(5-(5,7-dihydroxy-4-oxo-4*H*-chromen-2-yl)-2-methoxyphenyl)-5,7-dihydroxy-2-(4-methoxyphenyl)-4*H*-chromen-4-one (16)

Compound **16** was prepared according to the following procedure: to a suspension of **15** (50 mg ; 0.05 mmol ; 1.0 equiv.) in MeOH (2 mL) was added a few of DCM until all the product was dissolved. Then were added Pd/C 10 % (5 mg) and $Pd(OH)_2$ (5 mg). The mixture was purged with dihydrogen and stirred under atmosphere of dihydrogen for 5 hours at room temperature. The suspension was filtered on a celite pad and washed with a mixture of DCM/MeOH. The filtrate was condensed under reduced pressure and the resulting crude was purified by chromatography on a preparative TLC (DCM/MeOH: 94/6) to yield **16** as a pale yellow solid (21 mg ; 0.04 mmol; 75 %). **M.p.**: 219-221°C. **^{1}H NMR** (300 MHz, $CDCl_3$ and Methanol-d_4) δ (ppm): 7.99 (d, *J* = 8.6 Hz, 1H), 7.89 (d, *J* = 2.0 Hz, 1H), 7.46 (d, *J* = 8.6 Hz, 2H), 7.18 (d, *J* = 8.6 Hz, 1H), 6.81 (d, *J* = 8.6 Hz, 2H), 6.57 (d, *J* = 2.9 Hz, 2H), 6.42 (s, 1H), 6.38 (s, 1H), 6.23 (s, 1H), 3.78 (s, 3H), 3.76 (s, 3H). **^{13}C NMR** (75 MHz, DMSO-d_6) δ (ppm): 182.0, 181.7, 164.1, 163.9, 163.3, 163.0, 162.2, 161.1, 161.5, 160.6, 160.4, 160.3, 157.4, 154.3, 130.8, 128.1, 127.7, 122.8, 122.5, 121.6, 114.5, 111.7, 103.8, 103.6, 103.2, 98.8, 98.6, 94.0, 55.8, 55.4. **HRMS** (ESI^+): calculated for $C_{32}H_{23}O_{10}$ $[M+H]^+$ 567.1286; Found 567.1292. Spectroscopic data are consistent with literature data[28].

T-cell activation assay

MCA205 fibrosarcoma cells were transfected with the plasmid YFP-Globin-SL8-intron or with the PCDNA3 empty plasmid as described previously (REF). Twenty-four hours after transfection, cells were treated with different doses of Zardaverine (Merk Millipore) or IP2 (15µM) for 18h. Cell were then washed three times with PBS 1X and $5x10^4$ cells were co-cultured with $1x10^5$ SL8/H-$2K^b$-specific B3Z $CD8^+$ T-cell hybridoma for 18h at 37°C with 5% CO_2 overnight. Cells were centrifuged at 1200rpm for 5min, washed twice with PBS 1X and lysed for 5min at 4°C under shaking. Lysis buffer was composed of 0.2% TritonX-100, 10mM DTT, 90 mM K_2HPO_4, 8,5 mM KH_2PO_4. The lysates were centrifuged at 3000rpm for 10min to pellet cell debris and the supernatants were transferred to a 96-well optiplate (Packard Bioscience,

Randburg, SA). A revelation buffer containing 10 mM $MgCl_2$, 11,2 mM β-mercaptoethanol, 0,0015% IGEPAL® CA-630 et 40 µM 4-Methylumbelliferyl β-D-Galactopyranoside (MUG) was added and the plate was incubated at room temperature for 3 hours. Finally, β-galactosidase activity was measured using the FLUOstar OPTIMA (BMG LABTECH Gmbh, Offenburg, Germany).

Methodology to determine the Immunogenic cell death hallmarks

Cell lines and cell culture.

Human osteosarcoma U2OS cells were purchased from ATCC. U2OS cells stably expressing HMGB1-GFP together with H2B-RFP and CALR-GFP together with H2B-RFP were provided by Pr. Kroemer's group. U2OS cells were cultured in Dulbecco's modified Eagle's medium (Thermo Fisher Scientific) supplemented with 10% fetal bovine serum (Gibco by Life Technologies), 1% non-essential amino acids (Thermo Fisher Scientific), and 1% HEPES (Thermo Fisher Scientific) in a humidified incubator with 5% CO_2 at 37°C. For U2OS co-expressing HMGB1-GFP and H2B-RFP, 5 µg/mL blasticidin and 0.5 mg/mL G418 were added to the culture medium, while for U2OS co-expressing CALR-GFP and H2B-RFP the medium was supplemented with 5 µg/ml zeocin and 0.5 mg/mL G418. All cell lines were regularly tested for the absence of mycoplasma contamination.

Image acquisition and analysis.

For automated fluorescence/transmitted light microscopy, an ImageXpress confocal automated bioimager (Molecular Devices, San Jose, CA, USA), equipped with adequate excitation and emission filters (Semrock, Rocherster, NY, USA) and a 20X PlanAPO objective (Nikon, Tokyo, Japan) was used to acquire a minimum of four view fields per well.. For live cellular imaging, the atmospheric environment was controlled by an Ibidi gas mixer (Gräfelfing, Germany). The images were segmented and analyzed with the freely available software R (), integrated with the EBImage package from the Bioconductor repository (https://www.bioconductor.org), the MetaxpR package (https://github.com/kroemerlab/MetaxpR), the RBioFormats package (https://github.com/aoles/RBioFormats), as well as the MorphR package (https://github.com/kroemerlab/MorphR). Nuclei deep-learning based classification was performed using tensorflow and keras packages (https://cran.r-project.org/), allowing the application of pre-trained hdf5 models.

HMGB1 release and CALR translocation by live time-lapse imaging.

Two thousand U2OS cells per well stably co-expressing either HMGB1-GFP and H2B-RFP or CALR-GFP and H2B-RFP were seeded in 384-well µClear imaging plates (Greiner Bio-One) and let adhere for 24 h. The day after, cells were treated and HMGB1-GFP and CALR-GFP immediately after observed by live-cell microscopy with a frequency of image acquisition of one image every 1.5 h for 12 and 24 h, respectively. Images were then segmented and analyzed with R.

For the nuclei segmentation, H2B-RFP was used and the obtained mask was either employed for HMGB1-GFP to measure green fluorescence intensity in the nuclear compartment or as a seed to segment the cytoplasmic compartment using a Voronoi-based method for CALR-GFP. The coefficient of variation (CALR CV), defined as the ratio between fluorescence standard deviation and mean, was then computed. Cells were tracked and linked over time based on

their area and coordinates using the trackdem package. For each tracked cell, the difference of HMGB1-GFP nuclear fluorescence intensity between two time points was calculated.

Transcription inhibition assessment by deep-learning.
One day before treatment, two thousand five hundred U2OS cells were seeded in 384-well μClear imaging plates (Greiner Bio-One) and let adhere. The following day, cells were treated with drugs for 4 h. After fixation with 3.7% formaldehyde, transmitted light images were acquired and a dual deep-learning algorithm was applied to classify cells based on their nuclear phenotype, as described.[21] Briefly, cell nuclei were first segmented using a pre-trained Fully Convolutional Neural Network (FCNN), allowing the extraction of single-cell patches, and thereafter classified using a Deep Convolutional Neural Network (DCNN) in a binary fashion as "inhibited" or "control" phenotypes. The percentage of "inhibited" nuclei was finally calculated in each well and reported.

Transcription inhibition assessment by EU incorporation.
Evaluation of transcription was assessed by measuring the incorporation of Click-iT chemistry-detectable 5-ethynyl uridine (EU) (C10327, Thermo Fisher Scientific)[29] and according to the manufacturer's instructions. Two thousand five hundred U2OS cells per well were seeded in 384-well μClear imaging plates (Greiner Bio-One) and let adhere. The following day, cells were pre-treated for 2.5 h with drugs and then the treatment pursued in the presence of 1 mM 5-ethynyl uridine (EU) for an additional hour. Then, cells were fixed with 3.7% formaldehyde containing 1 μg/mL Hoechst 33342 for 1 h, permeabilized with 0.1% Triton X-100 for 10 min and unspecific binding was blocked by incubation with 2% BSA for 1 h at room temperature. The Alexa-Fluor-488-coupled azide was then added for 2 h at room temperature. The EU intensity corresponding to the GFP signal in the nucleus was measured by fluorescence microscopy and nuclear GFP values of each condition were normalized to the untreated control.

Transcription inhibition assessment by SYTO RNA staining.
Evaluation of transcription was measured by SYTO RNASelect green fluorescent cell stain (S32703, Thermo Fisher Scientific). Two thousand five hundred U2OS cells per well were seeded in 384-well μClear imaging plates (Greiner Bio-One) and let adhere. The following day, cells were treated with drugs for 4 h and fixed in methanol at -20°C for 10 min. The labelling solution consisting in 500 nM RNASelect green fluorescent cell stain in PBS was applied to cells immediately after preparation and incubated for 20 min at room temperature. After washing, nuclei were counterstained with 1 μg/mL Hoechst 33342 and images were acquired via confocal microscopy. Single GFP nuclei patches were then generated based on Hoechst staining and classified using a DCNN model pre-trained for SYTO-based transcription inhibition detection. The percentage of "inhibited" nuclei was finally calculated in each well and reported.

ATP release by quinacrine staining.
One day prior treatment, two thousand U2OS cells per well were cultured in 384-well μClear imaging plates (Greiner Bio-One) and let adapt. The next day, cells were treated with drugs for 24 h. Subsequently, in order to detect ATP enriched vesicles, cells were labeled with the fluorescent dye quinacrine as described.[30] In brief, cells were incubated with 5 μM quinacrine and 1 μg/mL Hoechst 33342 in Krebs-Ringer solution (125 mM NaCl, 5 mM KCl, 1 mM $MgSO_4$,

0,7 mM KH_2PO_4, 2 mM $CaCl_2$, 6 mM glucose, and 25 mM HEPES, pH 7.4) for 30 min at 37°C. Thereafter, cells were rinsed with Krebs-Ringer solution and live images were acquired via fluorescence microscopy. Quinacrine green fluorescence intensity was quantified in the cytoplasmic region and data were normalized to the control condition.

Statistical analysis.

Each experiment, one representative being depicted, contained 4 replicates of each condition from which mean and standard deviation were calculated. Statistical significance was assessed by means of a pairwise Welch Student's t-test against appropriate control.

***In vivo* experimentation:**

MTD determination:

To determine the maximum tolerated dose (MTD), the weight was the principal endpoint. Mice weight was followed every 48 hours. Euthanasia criteria included weight loss ≥20%, and in such cases the previous identified safe dose was set as the MTD.

Mice were injected intraperitoneally with 100µL of IP2 at four different concentrations once. The molecule IP2 was diluted at 50 mg/kg, 100 mg/kg, 250 mg/kg and 500 mg/kg in sterile phosphate–buffered saline (PBS).

Tumor challenge and drug treatment:

Female wild-type C57BL/6 mice at the age of 6 weeks were obtained from Harlan France. NU/NU nude mice were obtained from Charles River France. Animal experiments were conducted in compliance with the EU Directive 63/2010, and protocols 2016_064_5677 and were approved by the Ethical Committee of the Gustave Roussy Campus Cancer (CEEA IRCIV/IGR no. 26, registered at the French Ministry of Research). Mice were challenged subcutaneously in the right flank with $1x10^5$ MCA205 wild type (WT). For intravenous injection, from day 7 post inoculation and every 5 days until day 17, the mice were injected with 2,5mg/kg of IP2. For Intratumoral injection, from day 7 post cell inoculation mice were injected three times per week for two weeks with 5mg/kg of IP2. Area of the tumor was recorded every 3 to 4 days until ethical limit points were reached.

Cell culture and proliferation assay

Cancer cell lines were obtained from the American type Culture Collection (ATCC, Rockville, MD) or from the German collection of microorganism and cell culture from the Leibniz Institute (DSMZ, Braunschweig- Germany). Cancer cell lines were cultured according to the supplier's instructions. Human HCT-116 colorectal carcinoma were grown in Gibco McCoy's 5A supplemented with 10% fetal calf serum (FCS) and 1% glutamine. K562 myelogenous leukemia.

Cell lines were maintained at 37 °C in a humidified atmosphere containing 5% CO_2. Cell viability was determined by a luminescent assay according to the manufacturer's instructions (Promega, Madison, WI, USA). For IC_{50} determination, the cells were seeded in 96-well plates (3 × 103 cells/well) containing 100 µL of growth medium. After 24 h of culture, the cells were treated with the tested compounds at 10 different final concentrations. Each concentration was obtained from serial dilutions in culture medium starting from the stock solution. Control cells were treated with the vehicle. Experiments were performed in triplicate.

After 72 h of incubation, 100 µL of CellTiter Glo Reagent was added for 15 min before recording luminescence with a spectrophotometric plate reader PolarStar Omega (BMG LabTech). The dose-response curves were plotted with Graph Prism software and the

IC_{50} values were calculated using the Graph Prism software from polynomial curves (four or five-parameter logistic equations).

Plasma protein binding assay of IP2

IP2 plasma protein binding was determined in triplicate at 2 µM using the Rapid Equilibrium Dialysis (RED) Device Single-Use Plate with Inserts, 8K MWCO and associated protocol (ThermoFisher Scientific). LC-MS/MS system consisted on a Waters ACQUITY UPLC® System with a BEH Phenyl 1.7 µm, 2.1x50 mm column and a reversed phase gradient over a run time of 6 minutes. A mix of mobile phase A (ammonium formate 6mM pH5- 1,5-DMHA 20mM / Water ; 1/1; v/v) and mobile phase B (ammonium formate 6mM pH5- 1,5-DMHA 20mM / acetonitrile ; 1/1; v/v) were used at a flow rate of 0.6 mL/min and a column temperature of 50°C. The gradient conditions ramped from 20% B to 100% B between 0.5 and 4.5 min, then from 100% B to 20% B between 4.5 and 5.0 min, ramped to 20% B at 5.01 min and maintained up to 6.0 min for re-equilibration. The mass spectrometry analysis was performed on a Waters XEVO™ TQ-MS Mass Spectrometer operating in positive ion electrospray MRM mode with iP2 transition monitored as *m/z* 727 >567. In these conditions mean retention times was around 2.7 min.

■ ASSOCIATED CONTENT

Supporting Information

The Supporting Information is available free of charge at

1H and 13C NMR and ^{81}P NMR spectra for compounds 1a, **1b**, **2**, **3**, **M2P2**, **IP2** and **4-16**, purity LC-MS analysis of **IP2**, pharmacokinetic profile of IP2 (*iv* dog), *in vitro* immunogenic cell death induction by Isoginkgetin and IP2 harvested organs after injection of increased dose of IP2.

■ AUTHOR INFORMATION

Notes

The authors declare the following competing financial interest(s): S. A., D. R. and M. A. are inventors in the patent N° WO2018/189210 claiming compound IP2 disclosed in this paper, owned by CNRS, Inserm, University of Paris-Saclay and Gustave Roussy.

Corresponding Authors

Samir Messaoudi- Université Paris-Saclay, CNRS, BioCIS, 92290, Châtenay-Malabry, France,

Email : samir.messaoudi@universite-paris-saclay.fr

https://orcid.org/0000-0002-4994-9001

Sebastien Apcher - Université Paris-Saclay, Institut Gustave Roussy, Inserm, Immunologie des tumeurs et Immunothérapie, 94805, Villejuif, France.

Email : sebastien.apcher@gustaveroussy.fr

https://orcid.org/0000-0002-4434-5022

Authors Contributions

This manuscript was written through contributions of all authors. All authors have given approval to the final version of the manuscript.

■ ACKNOWLEDGMENTS

This work was funded by the FRM, project code n° DCM20181039530, La Fondation ARC, and Fondation Gustave Roussy.

ABBREVIATIONS

PDL1, Programmed death-ligand 1; CTLA4, Cytotoxic T-Lymphocyte Associated Protein 4; TNF-α, Tumor necrosis factor alpha; PTPs, pioneer translation products; NF-κB, nuclear factor kappa-light-chain-enhancer of activated B cells; MTT, 3-(4,5-dimethylthiazol-2-yl)-2,5-diphenyl-2H-tetrazolium bromide; HUVEC, Human umbilical vein endothelial cells; ADRB1, Adrenoceptor Beta 1; HRH2, Histamine Receptor H2; OPRD1, Opioid Receptor Delta 1; COX1, Cytochrome c oxidase I, PDE3A, Phosphodiesterase 3A; HEK293, Human embryonic kidney 293 cells; hERG, human ether-a-go-go-related gene; DAMPs, Damage-associated molecular patterns; MTD, Maximum tolerated dose.

■ REFERENCES

[1] Smith, A. J. New horizons in therapeutic antibody discovery: opportunities and challenges versus small-molecule therapeutics *J. Biomol. Screening* **2015***, 20,* 437–453

[2] Sampaio, E.P.; Sarno, E.N.; Galilly, R.; Cohn, Z.A.; Kaplan, G. Thalidomide selectively inhibits tumor necrosis factor alpha production by stimulated human monocytes. *J. Exp. Med*., **1991**, 173, 699–703.

[3]. Haslett, P.A.; Corral, L.G.; Albert, M.; Kaplan, G. Thalidomide costimulates primary human T lymphocytes, preferentially inducing proliferation, cytokine production, and cytotoxic responses in the CD8+ subset. *J. Exp. Med*., **1998**, *187*, 1885–1892.

[4] Quach, H.; Ritchie, D. Stewaet, A.K.; Neeson, P.; Harrison, S.; Smyth, M.J.; Prince, H.M. Mechanism of action of immunomodulatory drugs (IMiDS) in multiple myeloma. *Leukemia*, **2010**, *24*, 22–32.

[5] Buchbinder, E.; Desai, A. CTLA-4 and PD-1 Pathways: similarities, differences, and implications of their inhibition. *Am. J. Clin. Oncol*., **2016**, *39*, 98–106.

[6] Yewdell, J.; Anton, L.C.; Bennink, J.R. Defective ribosomal products (DRiPs): a major source of antigenic peptides for MHC class I molecules?. *J. Immunol*., **1996**, *157*, 1823–1826.

[7] a) Apcher, S.; Millot, G.; Daskalogianni, C.; Scherl, A.; Manoury, B.; Fåhraeus, R. Translation of pre-spliced RNAs in the nuclear compartment generates peptides for the MHC class I pathway. *Proc Natl Acad Sci USA*., **2013**, *110*, 17951–17956; b) Apcher, S.; Daskalogianni, C.; Lejeune, F.; Manoury, B.; Imhoos, G.; Heslop, L.; Fåhraeus, R. Major source of antigenic peptides for the MHC class I pathway is produced during the pioneer round of mRNA translation. *Proc. Natl. Acad. Sci. USA*., **2011**, *108*, 11572–11577.

[8] a) Tsalikis, J.; Abdel-Nour, M.; Farahvash, A.; Sorbara, M.; Poon, S.; Philpott, D.; Girardin, S. Isoginkgetin, a natural biflavonoid proteasome inhibitor, sensitizes cancer cells to apoptosis via disruption of lysosomal homeostasis and impaired protein clearance. *Mol. Cell. Biol*., **2019**, *39*, e00489–18. b) Li, P.; Zhang, F.; Li, Y.; Zhang, C.; Yang, Z.; Zhang, Y.; Song, C. Isoginkgetin treatment attenuated lipopolysaccharide-induced monoamine neurotransmitter deficiency and depression-like behaviors through downregulating p38/NF-κB signaling pathway and suppressing microglia-induced apoptosis*. J. Psychopharmacol*., **2021**, 1–15.

[9] Yoon, S. O.; Shin, S.; Lee, H. J.; Chun, H. K.; Chung, A. S. Isoginkgetin inhibits tumor cell invasion by regulating phosphatidylinositol 3-kinase/Aktdependent matrix metalloproteinase-9 expression. *Mol. Cancer Ther.* **2006**, *5*, 2666–2675.

[10] O'Brien, K.; Matlin, A.; Lowell, A.; Moore, M. The biflavonoid isoginkgetin is a general inhibitor of Pre-mRNA splicing*. J. Biol. Chem*., **2008**, *283*, 33147–33154.

[11] Pawellek, A.; McElroy, S.; Samatov, T.; Mitchell, L.; Woodland, A.; Ryder U, Gray D, Lührmann, R.; Lamond, A. I. Identification of small molecule inhibitors of pre-mRNA splicing. *J Biol Chem*. **2014,** *289*, 34683–34698.

[12] Darrigand, R.; Pierson, A.. Rouillon, M.; Renko, M. Boulpicante, M.; Bouyssié, D.; Mouton-Barbosa, E.; Marcoux, J.; Garcia, C.; Ghosh, M.; Alami, M.. Apcher, S. Isoginkgetin derivative IP2 enhances the adaptive immune response against tumor antigens, *Commun. Biol*. **2021**, *4*, 269–273

[13] Zhao, Y.; Cai, L.; Sui, Q.; Lin, F.; Jiang, W.; Chen, J.; Lu, W.; Gao, Q. Facile synthesis of acacetin and its derivatives. *Bioorg. Med. Chem. Lett.* **2016**, *26*, 3577–3580.

[14] Yuan, H.; Ye, J.; Chen, H.; Zhao, Z.; Luo, X.; Zhang, W.; Sun, Q. Facile synthesis of norwogonin, isoscutellarein, and herbacetin. *Tetrahedron. Lett.* **2016**, *57*, 3389–3391.

[15] Kumazawa, T.; Kimura, T.; Matsuba, S.; Sato, S.; Onodera, J.-I. Synthesis of 8-C-glucosylflavones. *Carbohydrate Res.* **2001**, *334*, 183–193.

[16] Sun, L.; Quan, H.; Xie, C.; Wang, L.; HU, Y.; Lou, L. Phosphodiesterase 3/4 inhibitor zardaverine exhibits potent and selective antitumor activity against hepatocellular carcinoma both in vitro and in vivo independently of phosphodiesterase inhibition*. PLoS One*, **2014**, *9*:e90627.

[17] Pitt, J.; Kroemer, G.; Zitvogel, L. Immunogenic and non-immunogenic cell death in the tumor microenvironment. *Adv. Exp. Med. Biol*., **2017**, *1036*, 65–79.

[18] Fucikova, J.; Kepp, O.; Kasikova, L.; Petroni, G.; Yamazaki, T.; Liu, P.; Zhao, L.; Spisek, R.; Kroemer, G.; Galluzzi, L. Detection of immunogenic cell death and its relevance for cancer therapy. *Cell. Death. Dis*., **2020**, *11*, 1013–1026.

[19] Humeau, J.; Sauvat, A.; Kepp, O.; Kroemer, G. An unexpected link between immunogenic cell death and inhibition of gene transcription. *Oncoimmunology*, **2020**, *9*, 1792039.

[20] Humeau, J.; Sauvat, A.; Cerrato, G.; Xie, W.; Loos, F.; Iannantuoni, F.; Bezu, L.; Levesque, S.; Paillet, J.; Pol, J. ; Leduc, M.; Zitvogel, L. De Thé, H.; Kepp, O.; Kroemer, G. Inhibition of transcription by dactinomycin reveals a new characteristic of immunogenic cell stress*. EMBO Mol. Med*., **2020**, *12*, e11622.

[21] Sauvat, A.; Cerrato, G.; Humeau, J.; Leduc, M.; Kepp, O.; Kroemer, G. High-throughput label-free detection of DNA-to-RNA transcription inhibition using brightfield microscopy and deep neural networks*. Comput. Biol. Med*., **2021**, *133*, 104371–104380

[22] Larsen, M. T.; Kuhlmann, M.; Lykke Hvam, M.; Howard, K. A. Albumin-based drug delivery: harnessing nature to cure disease*, Mol Cell Ther*. **2016**; *4*: 3. doi: 10.1186/s40591-016-0048-8

[23] Zhao Y., Cai, L.; Lin, F.; Jiang, W.; Chen, J.; Lu, W.; Gao, Q. Facile synthesis of acacetin and its derivatives, *Bioorg. Med. Chem. Lett.,* **2016**, *26*, 3577–3580

[24] Yuan H.; Ye, J.; Chen, H.; Zhao, Z.; Luo, X.; Zhang, W.; Sun, Q. Facile synthesis of norwogonin, isoscutellarein, and herbacetin, *Tetrahedron. Lett*., **2016**, *57*, 6345–6348.

[25] Kumazawa, T.; Kimura, T.; Matsuba, S.; Sato, S.; Onodera, J. Synthesis of 8-C-glucosylflavones, *Carbohydr. Res*., **2001**, *334*, 183–193.

[26] Zheng, X.; Meng, W. D.; Qing, F. L. Synthesis of gem-difluoromethylenated biflavonoid via the Suzuki coupling reaction, *Tetrahedron. Lett*., **2004**, *45*, 8083–8085.

[27] Park, H.II.; Si, C.-L. Chen, J. Total synthesis of amentoflavone, *Med. Chem*., **2015**, *5*, 467–469.

[28] Zhou Z. and Fu C. A new flavanone and other constituents from the rhizomes of Cyperus rotundus and their antioxidant activities, *Chem. Nat. Compd*., **2013**, *48*, 963–965.

[29] Deng, J.; Tian, A. L.; Pan, H.; Sauvat, A.; Leduc, M.; Liu, P.; Zhao, L.; Zhang, S.; Chen, H.; Taly, V.; Laurent-Puig, P.; Senovilla, L.; Li, Y.; Kroemer, G.; Kepp, O. Everolimus and plicamycin specifically target chemoresistant colorectal cancer cells of the CMS4 subtype, *Cell death Dis.* doi: **2021**, 12:978. doi: 10.1038/s41419-021-04270-x

[30] Forveille, S.; Humeau, J.; Sauvat, A.; Fezu, L.; Kroemer, G.; Kepp, O. Quinacrine-mediated detection of intracellular ATP. *Methods Enzymol*., **2019**, *629*, 103–113.